Int J Earth Sci (Geol Rundsch) (2006) 95: 119–142
DOI 10.1007/s00531-005-0019-9

ORIGINAL PAPER

Katalin Báldi

Paleoceanography and climate of the Badenian (Middle Miocene, 16.4–13.0 Ma) in the Central Paratethys based on foraminifera and stable isotope (δ^{18}O and δ^{13}C) evidence

Received: 23 February 2004 / Accepted: 27 June 2005 / Published online: 5 October 2005
© Springer-Verlag 2005

Abstract Benthic foraminifera and stable isotopes analyses revealed changes emerging in the paleoceanographic scenery in the Paratethys. The percentage of inbenthic, oxyphylic taxa and diversity in the benthic foraminiferal assemblage showed increasing food supply (organic matter), decreasing oxygen level and growing stress on the sea floor. Oxygen isotopes measured in planktonic and benthic foraminifera pointed to strengthening stratification during the Badenian period. The carbon isotopes indicated intensified accumulation of light marine organic matter. This increasing stratification trend is especially pronounced by Late Badenian (13.5–13 Ma) when surface water oxygen isotope values are rather negative. A simple two-layer circulation model was worked out for the Badenian Paratethys explaining these characteristic environmental changes. An *antiestuarine (lagoonal)* circulation is assumed for the Central Paratethys during the Early (16.4–15 Ma) and mid Badenian (15–13.5 Ma). The mid Badenian period of time comprises the short episode of evaporite formation in the Carpathian Foredeep and the Transylvanian Basin. Evidence presented here supported a reversal of circulation to *estuarine* type after the deposition of salts by Late Badenian (13.5–13 Ma). The Early Badenian antiestuarine circulation is suggested to associate with the high temperatures of the Mid-Miocene Climatic Optimum, and the Late Badenian estuarine circulation with the cooler period following it.

Keywords Miocene · Paratethys · Stable isotopes · Foraminifera · Climate

K. Báldi
Department of Physical and Historical Geology,
Eötvös University Budapest, Pázmány Péter sétány 1/c,
1117 Budapest, Hungary
E-mail: kabaldi@ludens.elte.hu

Present address: K. Báldi
Department of Paleontology, Micropaleontology Research Group,
University of Vienna, Althanstrasse 14, 1090 Vienna, Austria

Introduction

Recent developments in reconstructing climate and paleoenvironment in the Central Paratethys region show evidence for an initially warm-temperate climate followed by a temperature decline in the Middle Miocene (Schwarz 1997; Vennemann and Hegner 1998; Gonera et al. 2000; Ivanov et al. 2002; Bicchi et al. 2003; Böhme 2003). It is generally accepted that this warm period and the subsequent cooling correlates with global climate changes well-known from the deep-sea record (Miller et al. 1991; Flower and Kennett 1994; Zachos et al. 2001). However, the intricate relationship between climate and circulation in the Paratethys, spreading from the Mediterranean to the Indo-Pacific (Fig. 1a), has not been considered.

In the Mediterranean the Neogene circulation has been studied in reasonable detail (Gebhardt 1999; Seidenkrantz et al. 2000; Kouwenhoven and Van der Zwaan; 2004, among others). The common approach of Paratethys researchers deals with connections between the Paratethys and nearby seas (Daniels and Ritzkowski 1970; Rögl et al. 1978; Rögl and Steininger 1983; Steininger and Rögl 1984; Por and Dimentman 1985; Martini 1990; Rögl 1998b). This approach is based on the distribution of sediments and similarity of marine faunas. Problems arise in such reconstructions when the absence of sediments indicates the existence of land, or erosional hiatuses destroying the marine record. Hardly has any author ventured from mapping the boundaries of these inland seas to reconstructing circulation and other aspects of oceanography. An exception is Kókay's (1985) attempt to understand better the circulation of the Late Badenian Paratethys.

According to paleogeographic reconstructions (Rögl et al. 1978; Steininger and Rögl 1984; Szczechura 1996; Rögl 1998b; Studencka et al. 1998; Meulenkamp and Sissingh 2003), the Paratethys consisted of a chain of seas situated between the Mediterranean and the Indo-Pacific during the Badenian (Middle Miocene:

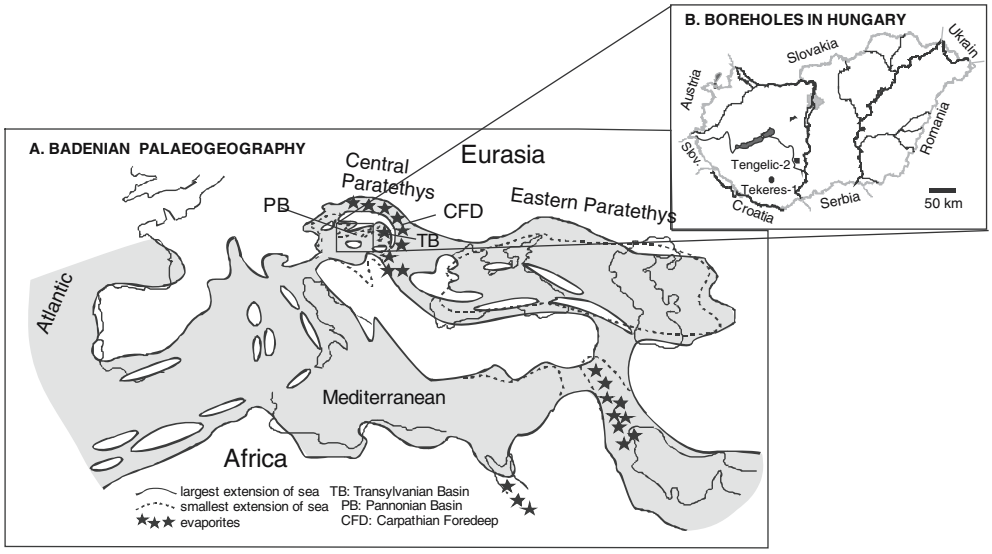

Fig. 1 A. Schematic map of Europe showing (in *solid line*) the maximum extension of the Paratethys through Badenian times, with all seaways open, communicating with the Mediterranean and the Indo-Pacific. The *dashed line* represents the smallest extension of the Paratethys through Badenian times. Black asterisks represent the mid Badenian evaporitic sediments forming a belt in the Outer Carpathians embracing the Transylvanian evaporite occurrence. The figure is after the palinspastic reconstructions of Rögl (1998b) and Steininger and Rögl (1984). B. Enlarged is the map of Hungary showing the location of the boreholes Tengelic-2 and Tekeres-1 (after Báldi et al. 2002)

Langhian, Serravallian, Fig. 1a). During the Early Badenian, a deep strait connected the Central Paratethys to the Mediterranean (Rögl et al. 1978; Steininger and Rögl 1984; Rögl 1998b).

In mid Badenian times widespread evaporites in the Carpathian Foredeep and Transylvanian Basin, relative sea-level drops and erosional hiatuses testify for tectonic activity (Filipescu and Girbacea 1997; Rögl 1998b; Báldi et al. 2002). However, in the Pannonian Basin no evaporites of mid Badenian age were found and no faunal evidence pointed towards increased salinity, which could have helped to correlate the time horizon of the salinity crisis within the entire Paratethys realm.

The Mediterranean character of the Early Badenian faunas in the Central Paratethys is emphasized by every author; however, opinions diverge about the Late Badenian faunas. The presence of Indo-Pacific faunal elements is stressed and the closure of the seaway towards the Mediterranean envisaged for Late Badenian time (Steininger and Rögl 1984; Rögl 1998b). Others assume an East Paratethys connection to exist with the Central Paratethys with a continuous Mediterranean water exchange during Late Badenian ''Konkian'' time (Kókay 1985; Szczechura 1996; Studencka et al. 1998). The idea of a transgression from the Eastern Paratethys in Late Badenian time is supported by the interpretation of seismic sections of the Carpathian Foredeep (Krzywiec 2001).

Stable isotopes are also rather rarely measured in Paratethys marine sediments of this age, while for the Mediterranean records see Vergnaud-Grazzini (1985) with a large published database and more recently Sprovieri et al. (1999). There are several studies from the Pannonian Basin focusing on the much younger Pannonian Lake (Geary et al. 1989; Mátyás et al. 1996). Mátyás et al. (1996) considered oxygen isotope measurements to be an unsuitable tool for salinity reconstructions of inland lakes due to instability of its oxygen isotope composition. The present study deals with the much older sediments of the predecessor of the Pannonian Lake, a widespread normal marine inland sea called Central Paratethys, and thus it was expected to find stable isotope data more useful. There are already isotope measurements from the Carpathian Foredeep part of the Paratethys carried out on samples of Badenian age (Gonera et al. 2000) as in the present study.

Benthic foraminifera are well-known tools for paleoenvironmental reconstructions. Their assemblages reflect the changes in environmental factors, like food and oxygen availability, in relation to the oceanologic regime of the Central Paratethys. Since the pioneer work of Corliss (1985) and Corliss and Chen (1988) in the 1980s, it is commonly accepted that microhabitat separation of benthic foraminifera is likely to have consequences for test morphology. This is manifested in the association of trochospiral test morphology with an epibenthic, and elongate, serial test morphology with an inbenthic microhabitat (see further references in Rosoff and Corliss 1992; De Stigter et al. 1998). There are numerous studies on the in-sediment depth distribution of present day living benthic foraminifera stained at the time of sampling (e.g. De Stigter et al. 1998; Fontanier et al. 2002). The particular depth of a species in the sediment is either mainly controlled by food supply under oligotrophic conditions or by oxygen availability under eutrophic conditions according to the

TROX-model of Jorissen et al. (1995). At the same time the shifting of the toxic redox front in the sediment is mentioned as an important factor for benthic foraminiferal life (Jannink et al. 1998; Den Dulk et al. 2000; Fontanier et al. 2002). Many authors have studied the complex relationship of benthic foraminiferal assemblages with organic flux or oxygen content of bottom waters (e.g. Kaiho 1994, 1999; Murray 2001; Altenbach et al. 2003). In the present study special attention was paid to epibenthic and inbenthic forms, anticipating that their number in the total assemblage reflects trophic conditions and stress.

With an aim to improve our understanding of the paleoceanography of the Central Paratethys finding well-preserved cores transecting the whole Badenian sequence in deeper-water facies recording the paleoceanographic events of the Central Paratethys in the Pannonian Basin was a challenging task. Finally two boreholes (Tekeres-1, Tengelic-2, SW Hungary) were selected for the quantitative analyses of foraminifera and stable isotope measurements (Fig. 1b), appreciating the relatively good preservation, unique in pelagic Badenian facies, and the detailed earlier studies carried out by the Geological Institute of Hungary (Hámor 1970; Halmai et al. 1982). The foraminiferal faunas of these cores were studied earlier to consider ideas on circulation without actual isotope measurements (Báldi 1997), to provide taxonomic description (Báldi 1999), and to reconstruct subsidence history of the region (Báldi et al. 2002). For the present study, foraminiferal data were re-evaluated and stable isotope measurements have been carried out on the same sample set for the first time from Badenian sediments of the Pannonian Basin. The foraminiferal and stable isotope evidence was combined in order to contribute to the better understanding of circulation of the Central Paratethys summarized in a model for the Badenian time period discussed in relation to global climate changes.

Stratigraphic framework and methods

Stratigraphy and lithology

Badenian stratigraphy and correlation of cores

The base of the regional Central Paratethys Badenian stage coincides with the start of the early Middle Miocene (the base of Langhian at 16.4 Ma) and it ends in the early Serravallian (~13 Ma) according to Rögl (1998a). The standard zonation of Martini (1971) is followed in the present work concerning nannofossil biostratigraphy. The boundary of the NN 5/ NN 6 nannozone is defined by the last occurence (LO) of *Sphenolithus heteromorphus*, which is generally dated around 13.5 Ma on the time scale of Berggren et al. (1995).

The Central Paratethys stage Badenian, by original definition, comprises the period of time between the first appearance (FA) of *Praeorbulina glomerosa* and the first characteristic Sarmatian mollusc fauna (Papp and Cicha 1978). Its definition relies heavily on mollusc and benthic foraminiferal stratigraphy, while correlating to nannozones is less straightforward. The Badenian begins in the nannozone NN 4 (Rögl 1998a; Rögl et al. 2002; Harzhauser et al. 2002) or with the onset of NN 5 (Steininger et al. 1990; Švabenická 2002) and ends during NN 6 (Rögl 1998a; Harzhauser et al. 2002) or at the end of NN 6 (Steininger et al. 1990: see Báldi et al. 2002 for comparing zonations). There is a regional Paratethys benthic foraminiferal zonation in use. According to this zonation the Badenian starts at the base of the Lower Lagenid Zone, followed by the Upper Lagenid Zone, the Agglutinated Zone, the *Bolivina – Bulimina* Zone, with the "Verarmung Zone" and " *Ammonia beccarii* Zone" heralding the onset of a new stage, the Sarmatian (Grill 1941; Papp et al. 1978).

The subdivision of the Badenian period is either bipartitional (Early and Late), or tripartitional (Early, Middle and Late) varying among authors. As the present work does not focus on stratigraphy the following simple concept is used to present data. The time span from the Karpatian/Badenian boundary to the NN 5/NN 6 boundary in our record is referred to as Early and mid Badenian, as in the studied interval record NN4 was missing (Nagymarosy 1982, 1985). Early and mid Badenian presented here is dated 16.4–13.5 Ma and referred to as NN 5 Badenian. The term mid Badenian is used for the time period comprising the short time interval (0.2 Ma according to Balintoni and Petrescu 2002) of the salinity crisis resulting in evaporite formation in the Carpathian Foredeep and the Transylvanian Basin. However, its correlation (Luczkowska 1979; Szczechura 1982; Mészáros et al. 1989; Marinescu and Mârunteanu 1990; Peryt 1997; Chira and Dragici 2002) with the Pannonian Basin and the marine record studied in this paper is impossible as evaporites of this age are absent in Hungary. Nevertheless special attention is paid to this time period because of the paleoceanographic importance of evaporite formation. The term Late Badenian in the present work refers to the period from the NN 5/NN 6 to the Badenian/Sarmatian boundary dated as 13.5–13 Ma time span (see Fig. 5a).

The time frame applied here is based on the nannoplankton zonation and stratigraphical summary provided by Nagymarosy (1982, 1985). The two studied boreholes (Tengelic-2, Tekeres-1, Fig. 1b) are correlated along the Karpatian/Badenian and the Badenian/Sarmatian boundaries based on mollusc and benthic foraminiferal zonation (Halmai et al. 1982; Nagymarosy 1982, 1985) and the NN 5/NN 6 nannozone boundary after Nagymarosy (1982, 1985, Fig. 2). Concerning Badenian/Sarmatian boundary Nagymarosy (1982, but not 1985) was followed as *Discoaster kugleri*'s occurrence is not accepted because of uncertainty of recognition. Detailed sedimentological description and subsidence history based on paleowater depth estimates obtained using foraminiferal planktonic/benthic ratio can be found in Báldi et al. (2002).

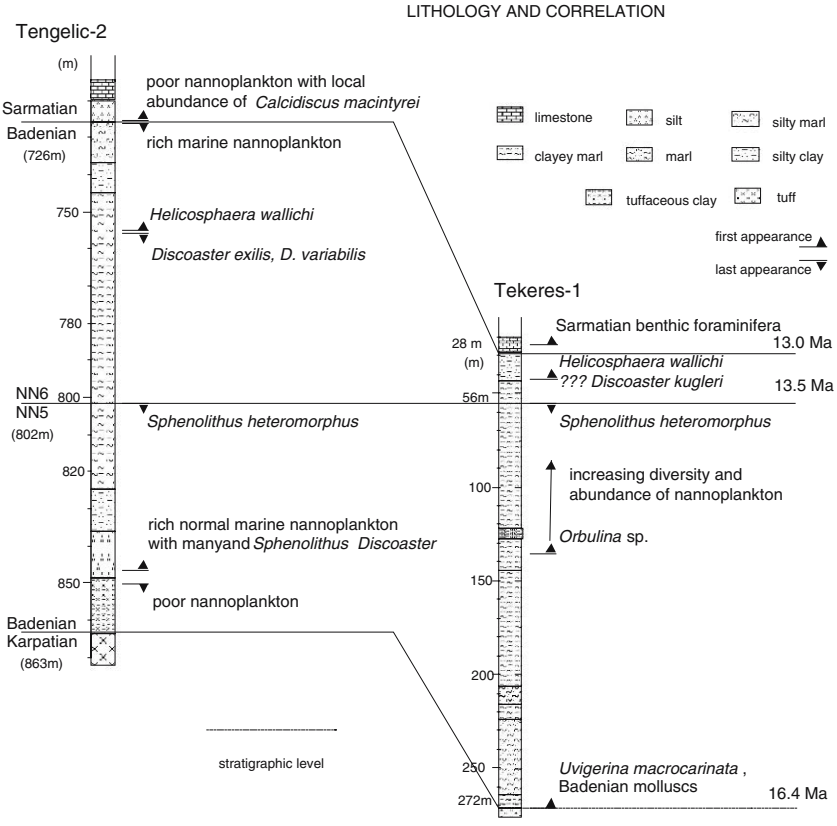

Fig. 2 Schematic lithologic columns and correlation of Tengelic-2 and Tekeres-1 boreholes (Halmai et al. 1982; Nagymarosy 1982, 1985). The cores are correlated along the Karpatian/Badenian and Badenian/Sarmatian boundaries based on mollusc and benthic foraminifera stratigraphy and the NN5/ NN6 nannoplankton zone. The age of the upper and lower boundaries of the Badenian on an absolute scale are taken from Rögl (1998a), the NN5/ NN6 boundary is based on Berggren et al. (1995). Distribution of stratigraphical markers in the cores is after Nagymarosy (1982, 1985)

Core description

The studied interval of Tengelic-2 (Fig. 2), which yielded benthic foraminifera in statistically significant numbers, ranged from 844 m to 738 m (samples w-a). Underlying there are effusive vulcanites and continental to brackish sediments. The first normal salinity marine beds containing NN 5 nannoflora (Nagymarosy 1982) occur at 847 m in sand. These beds are overlain by a sequence of lithofacies ranging from limestone to silt and silty clay (847–823 m) to become rather homogeneous clay-marl (823–746 m) and clayey silt layers (746–726 m). This part of the section contains the NN 5/NN 6 boundary at 802 m. Overlying the Badenian from 726 m upward are Sarmatian sediments based on appearance of characteristic macrofauna and impoverished nannoflora (Halmai et al. 1982; Nagymarosy 1982).

In borehole Tekeres-1 (Fig. 2) the studied Badenian sediments (276–47 m, samples MI-A) overlie silty clayey marls (328–272 m). The first fauna indicating normal marine conditions occurs at 365 m, with NN 5 nannoflora (Nagymarosy 1980, 1985) and marine macrofauna, followed by silty to clayey marls. The first characteristic Badenian benthic assemblages with *Uvigerina macrocarinata* and Badenian molluscs appear higher at 272 m (Nagymarosy 1980), from where samples were available for the present study. From 136 to 76 m a remarkable increase in both diversity and abundance of nannoflora was detected. Above (76–60 m) nannofossils almost disappear (Nagymarosy 1980, 1985) while the NN 5/NN 6 boundary was found at 56 m. According to Nagymarosy (1982), the Badenian/ Sarmatian boundary is at 28 m based on the appearance of Sarmatian benthic foraminifera. The uppermost part of the Badenian of the core was identified as NN7 (Rögl and Müller 1976) based on the presence of *Discoaster kugleri* (Nagymarosy 1985), whose zone was later correlated to the Sarmatian (Rögl 1996, 1998a among others). However, the recognition of *D. kugleri* is problematic due to overcalcification and rare presence in Paratethys. Thus there also the classical definition of the Badenian stage was followed based on benthic foraminifera, in spite of the observations of Nagymarosy (1985). Below the NN 5/6 boundary there is an indication of a depth increase by the appearance of more pelagic forms of nannofossils.

Samples and methods

Benthic foraminiferal counts

Planktonic and benthic foraminifera were picked from the 125–595 μm fraction after washing in water and wet-sieving, and splitting to the right size allowing to pick

Table 1 Counting results and calculations of core Tengelic-2. Inbenthic taxa are denoted by single asterisks, while oxyphylic taxa are denoted by double asterisks. The use of decimals is a result of counting broken tests or number of chambers making up a whole specimen. Calculated values plotted against depth in the core in Fig. 3 are typed in boldface

Tengelic-2 samples	Depth in core	*Allomorphina trigonia* (REUSS)*	*Ammonia beccarii* (LINNÉ)	*Asterogerina planorbis* (D'ORBIGNY)	*Astronomion cf. italicum* (CUSHMAN & EDWARDS)	*Bolivina antiqua* (D'ORBIGNY)*	*Bolivina hebes* (MACFADYEN)	*Bolivina plicatella* (CUSHMAN)	*Bolivina scalprata var. miocenica* (MACFADYEN)	*B. spathulata* (WILLIAMSON) *f. spathulata**	*B. spathulata* (WILLIAMSON) *f. dilatata**	*Bolivina trajectina* (MARKS)	*Bolivina viennensis* (MARKS)*	*Bolivina* undetermined	*Bulimina* sp.*	*Bulimina elongata* (D'ORBIGNY)*	*Bulimina costata* (D'ORBIGNY)	*Cancris auriculus* (FICHTEL & MOLL)	*Cassidulina crassa* (D'ORBIGNY)	*Cassidulina oblonga* (REUSS)*	*Cassidulina subglobosa* (BRADY)*	*Cassidulina laevigata* (D'ORBIGNY)	*Cassidulina teretis* (TAPPAN)	*Ceratocancris haueriana* (D'ORBIGNY)	*Chilostomella* sp.*	*Cibicides lobatulus* (WALKER & JACOB)**	*Cibicides kullenbergi* (PARKER)**	*Cibicides ungerianus* (D'ORBIGNY)**
a	738.45			1				3		1						74	42			2	6		1			13		5
b	743.8	1		6	1						2					16	17				4		1			18		6
c	749	1						3						1		17	28				6				1	13		10
d	754.05	2		2						1	1					19	39			12	6		1			10		17
e	759.9	2		2				2				1	15			30	20			3	2			7		8		3
f	764.5			7		1		1		1			4			26	18		2	7	2	1	1	1		3		2
g	768.85			1	1			1					9			12	33			5				1		9		8
h	773.75			1	1											14	49			2						8		3
ij	777.85			2	2			1	16				3			14	27			6			12	1		16		4
k	781.45		2	1				3	1				3		1	17	22	1		4	3	1				8		3
l	785.55	1	1	1				2	2				1			10	17			4		1		2		12		7
m	789.5	1						3	4				2			21	14			7	1	3	3		3	16		8
n	793	1	2	1				1					4		2	12	15		1	3	1		1		3	16		8
o	796.5		1	1	1								3		1	10	18			3	1					18		9
p	801.3			5	1											6	37			7	5	1			2	26		7
q	807.05	9						1					1	1		1	35	1							1	24		3
r	812.75	7		2				1					10			7	12		8	1	1	1			5	19		4
s	817.8	4							1							14	20								3	4		5
t1	823.4	6		9	4			3					36			36	27	1		1	3				2	29		15
t2	828.75	4		2	2			2	2				7			11				5	14				2	25		10
u	833.35			3	2	4	4	6	2				11			5	3			12	1				1	30		8
v	838.35				1	3	21						4			1						1	1	1		29	9	13
w	844		11	4		3	13		1				1	1		2	1			1	1	1	1			21	8	19

the statistically significant number of 200–300 specimens of benthic foraminifera. The very few foraminiferal specimens from the base of the marine sequence showing signs of resedimentation under the light microscope were excluded. The foraminifera were determined to the species level wherever possible, mounted on Chapman-slides, and counted (Tables 1, 2). The Fisher's alpha diversity was calculated using the formula given by Fisher et al. (1943), with the constants taken from Williams (1964, Fig. 125). This index compensates for different "sample sizes": the different number of benthic foraminifera picked from a given split. Diversity was interpreted as a measure of environmental stress displayed by the benthic assemblages.

Microhabitat distribution

The percentage of inbenthic foraminifera in the total benthic foraminiferal assemblage was calculated to learn more about the trophic conditions. Considering the importance of in-sediment distribution of benthic foraminifera in environmental reconstructions, it had to be established which species is to be considered inbenthic and which is to be considered epibenthic foraminifera. As a general rule trochospiral test morphology is associated with epibenthic, and elongate serial test morphology with inbenthic microhabitat (Corliss 1985; Corliss and Chen 1988; Rosoff and Corliss 1992; De Stigter et al. 1998). The actual in-sediment living depth

Table 1 (Contd.)

Coryphostoma schmidi (POPESCU)	*Dentalina* spp.	*Dentalina brevis* (D'ORBIGNY)	*Dentalina elegans* (D'ORBIGNY)	*Elphidium* spp.	*Epistominella* spp.	*Fissurina* sp.	*Fursenkoina acuta* (D'ORBIGNY)*	*Gavelinopsis praegeri* (HERON-ALLEN & EARLAND)	*Glandulina* sp.	*Globobulimina pyrula* (D'ORBIGNY)*	*Globulina* sp.	*Guttulina austriaca* (D'ORBIGNY)	*Guttulina communis* (D'ORBIGNY)	*Gyroidina parva* (CUSHMAN & RENZ)	*Gyroidina soldanii* (D'ORBIGNY)	*Gyroidina umbonata* (SILVESTRI)	*Hansawaia boueana* (D'ORBIGNY)	*Heterolepa dutemplei* (D'ORBIGNY)**	*Heterostegina* sp.	*Hoeglundina elegans* (D'ORBIGNY)	*Lagena* sp.	*Lenticulina calcar* (LINNÉ)**	*Lenticulina arcuata* (D'ORBIGNY)**	*Lenticulina* sp.**	*Melonis barleeanum* (WILLIAMSON)*	*Melonis pompilioides* (FICHTEL & MOLL)*	*Adelosina* sp.	*Pyrgo?* sp	*Quinqueloculina* sp.
				2				21				1			6		18	6					3		3	7			
						1		10	2	1		1	1		2	7	7	7	1		2		1		6	9			
				1			1	14		7		2	2		10	2	8	3					1		5	3			
1				1	1			14		2					2	3	9	6			4				1	3			
					3		2	4		5					8	2	8	2		9	2				1	6			1
				3	3			3		2			1	1	1		17	2		4						3			7
				2	3	1	5	1		4					4	3	9	4		4	2		1	1		8			6
					9	1	4	7		4		3		1	2	2	2	11			3					2			1
				1	2			10		5		1			2	2	11	3		3	2				4	1			2
					4	1	2	2		4	2	2			6	1	10	6		1	3		1		2	6	1		
					3		3	4		2		2			4	4	3	8		2	6			1	1	4			5
				2	3		7	3		5			1		2	3	7	6		1			1	1		3			2
				1	1		3	1		19					21	2	5	7			3				2	2	1		12
	0,3			1	2	1	1	1		3		4			5	2	3	16		2	6		1	1		3			3
	0,5			1	8			2		3		1			6	3		10			4			2		8			4
	0,6			3	1	2				8		1			1	1	2	14			9			2	2	6	1	4	3
	1,4		4				1	1		3		2					7	19			8			1		10			5
				1	2		4	4		6					2	2	3	9			10					3		3	1
			3		8		5	9	3	8			1		2	3	11	16			7			1	6	17		1	2
	0,1		1	1			1								5	7	12	11			6				4	3		1	2
						2	3	4		3		3			1	8	14	12			3	3		7	4	6		1	
		1	8				1								8	1	4	23			1	2		6	2	7		1	
	0,6		17	10											5	3	2	36			11			7		13		1	

in the present day seas reported for a particular species by different authors served as a guideline too (Rathburn et al. 1996; Den Dulk et al. 2000; Fontanier et al. 2002 among others). Tables 1 and 2 list the inbenthic species (denoted by one asterisk).

The morphological criteria for an infaunal life-mode were carefully considered at the species level. Generally all species belonging to the elongate, smooth and serial shaped genera, non-endemic *Bolivina*, non-costate *Bulimina*,*Uvigerina*, *Fursenkoina*, and *Globobulimina* were considered to be infaunal. Among the excluded endemic bolivinids *B. viennensis* resembling *B. spathulata* was considered infaunal (see *B. spathulata* under the name *B. dilatata*, deep infaunal in De Stigter et al. 1998; Den Dulk et al. 2000). The closely related *Cassidulina subglobosa* and *C. oblonga* (perhaps ecophenotypic variations, Báldi 1999) were regarded as infaunal here, where as *C. subglobosa* was classified as "intermediate infaunal" (Den Dulk et al. 2000). The taxa *Allomorphina trigona* and *Chilostomella* sp., rare in the material, are very likely to have an infaunal microhabitat based on their morphology (see *Chilostomella oolina* deep or intermediate infaunal in Rathburn et al. 1996; Fontanier et al. 2002). The species *Melonis barleeanum, Pullenia quinqueloba* and *Sphaeroidina bulloides* are generally found to vary from shallow to intermediate infaunal

Table 1 (Contd.)

Spirolocullina excavata (D'ORBIGNY)	*Spirolocullina badenensis* (D'ORBIGNY)	*Miliolid* spp.**	*Nodosaria* sp.1	*Nodosaria* sp.2	*Nodosaria raphanistrum* (LINNÉ)	*Nonion commune* (D'ORBIGNY)	*Nonionella turgida* (WILLIAMSON)	*Oridorsalis umbonatus* (REUSS)	*Planulina* sp.	*Pullenia bulloides* (D'ORBIGNY)*	*Pullenia quinqueloba* (REUSS)*	*Reusella spinulosa* (REUSS)	*Siphonina reticulata* (CZJEK)**	*Sphaeroidina bulloides* (D'ORBIGNY)*	*Stilostomella adolphina* (D'ORBIGNY)	*Trifarina angulosa* (WILLIAMSON	*Trifarina bradyi* (CUSHMAN)	*Uvigerina hispida* (SCHWAGER)*	*Uvigerina semiornata* (D'ORBIGNY)*	*Uvigerina pygmea* (D'ORBIGNY)*	*Uvigerina venusta* (FRANZENAU)*	*Uvigerina aculeata* (D'ORBIGNY)*	*Uvigerina acuminata* (HOSIUS)*	*Uvigerina* spp.*	*Vaginulopsis pedum* (D'ORBIGNY)	*Valvulineria complanata* (D'ORBIGNY)*	Undetermined calcareous specimens	*Haplophragmoides* sp.
						1	1			39				11		3		1	8							9		1
			1			22				26		1		11				3	9					3		5	2	2
						10				33				6		7		1	16		1					9	1	
			0.5			43		3		8				5		1			4		4					2	3	
						32		1		15		1		1	0.2			1	6							2	4	1
						78				12				1					2			11				1	3	3
		4				44		1		3									4			7				1	7	
			0.5			29				9									10			3				3	3	4
						44		1		8				4					15		4						4	
						27		1		16				3	1				7							2	3	1
						35				13				4		1			15	6				8		2	4	1
						38		2		11				4					14		5	3				4	5	1
		5	2.5			10				8			1	2					5			3				5	3	1
			1.5			14				15	2			1					16		1	2					3	4
		1	0.5			17				6				4	1				10								3	1
		2	3	3		5	1			10				8	6				4			15				2	5	6
		2	5	4		7				17				4	5				3			7		5		8	5	2
		4		4	8	24	2	2		15				2	1				5			3		4		3	10	1
	2		1	9	1	16		1		19	1		3	2	2				3			1		1	1	24	10	
	1	2	0.5	2			2	2		8	1		5	2		1							5	7		7	11	
1	1					3				2	2		4		1		1		8	1			1	4		10	2	
	1		1.5				1	1	10	2	1		10	3	2		1						19	13			5	
	2		1	2		4			15	5			19	4	3	1	1					12	23	8			6	

(Rathburn et al. 1996; De Stigter et al. 1998; Den Dulk et al. 2000; Fontanier et al. 2002) and were included among the infaunal taxa. Based on the literature concerning the distribution of *Melonis barleeanum* and *Pullenia quinqueloba*, the morphologically very similar *M. pompilioides* and *P. bulloides* were considered infaunal also. *Valvulineria complanata*, synonymous to *V. bradyana*, shows preference for organic-rich substrates in the present day Adriatic Sea (Jorissen 1987) and the similar *V. mexicana* is deep infaunal (Rathburn et al. 1996).

Reconstruction of bottom water conditions concerning oxygen content was based on the presence of oxic indicators or oxyphylic species in the assemblage. Several methods were developed to tie changes in the benthic foraminiferal assemblages to actual dissolved oxygen levels of the bottom water, like the BFOI index (Kaiho 1994, 1999). Here, for practical reasons the work of Kouwenhoven and Van der Zwaan (2004) was also followed. A simplified method was used here, summing the percentages of oxyphylic or oxic taxa (“group 5” in Kouwenhoven and Van der Zwaan, 2004 or “oxic indicators” defined as >1.5 ml/l oxygen content in Kaiho 1994) in each sample to reflect bottom water conditions. Tables 1 and 2 list the oxyphilic species (denoted by two asterisks).

The selection of strictly epibenthic, oxyphylic species was done with special care. Such species inhabit the topmost sediment layer, where oxygen is available in excess. This microhabitat of foraminifera in the sediment column shifts with the anoxic front (Van der Zwaan and Jorissen 1991; Kaiho 1994; Jorissen et al. 1995; De Stigter et al. 1998) and with the toxic front (Jannink et al. 1998; Den Dulk et al. 2000; Fontanier et al. 2002). All *Cibicides* species (including *Heterolepa dutemplei* synonymous to *Cibicides dutemplei*) were considered oxic

Table 1 (Contd.)

Martinotiella communis (D'ORBIGNY)	*Spiroplectammina carinata* (D'ORBIGNY)	*Textularia* sp.	*Textularia cf. mexicana*	*Sigmoilopsis* sp.	Undetermined agglutinated specimens	Total number of benthic	Number of inbenthic *	**Percentage of inbenthic****	Corrected number of benthic	Number of planktonic foraminifera	Percentage of planktonic	Percentage of plankontic corrected for inbenthic	**Estimated paleowater depth (m)**	Counting listed taxa	Number of species including spp. and undet.	**Fisher's alpha diversity**	Number of oxyphyl taxa**	**Percentage of oxyphyl taxa****
1.8	15			4		309.8	161	**52.0**	148.8	58	15.8	28.0	**97.4**	31	31	**8.6**	27	**8.7**
2.1	11		2			230.1	94	**40.9**	136.1	56	19.6	29.2	**101.2**	39	39	**13.5**	32	**13.9**
3	14			3		243.0	107	**44.0**	136.0	73	23.1	34.9	**124.2**	34	34	**10.8**	27	**11.1**
1.25	3			2	2	238.8	69	**28.9**	169.8	80	25.1	32.0	**112.1**	37	37	**12.3**	33	**13.8**
2.2	17	1	3	2	5	242.4	91	**37.5**	151.4	70	22.4	31.6	**110.4**	42	42	**14.7**	13	**5.4**
	15	3	2	2	2	259.0	73	**28.2**	186.0	52	16.7	21.8	**78.2**	40	40	**13.2**	7	**2.7**
0.2	6.5		11	1	2	229.7	58	**25.3**	171.7	128	35.8	42.7	**163.5**	39	43	**15.6**	27	**11.8**
0.3	13			3	8	215.8	51	**23.6**	164.8	76	26.0	31.6	**110.2**	33	37	**12.9**	22	**10.2**
0.2	5		2	1	5	246.2	64	**26.0**	182.2	73	22.9	28.6	**99.3**	38	41	**14.0**	23	**9.3**
1	10	2	5	8	4	215.0	70	**32.6**	145.0	58	21.2	28.6	**99.2**	46	46	**17.9**	18	**8.4**
2	3	3		1		211.0	74	**35.1**	137.0	51	19.5	27.1	**94.2**	42	44	**16.9**	28	**13.3**
1	5	1	5	2	1	235.0	91	**38.7**	144.0	166	41.4	53.5	**239.7**	44	47	**17.7**	32	**13.6**
4	7	5	12	1	6	231.5	75	**32.4**	156.5	239	50.8	60.4	**305.8**	46	52	**20.9**	37	**16.0**
6	10		4	2	10	212.5	62	**29.2**	150.5	95	30.9	38.7	**141.8**	43	49	**19.9**	45	**21.2**
	4.5		4			201.0	51	**25.4**	150.0	89	30.7	37.2	**134.7**	33	37	**13.3**	46	**22.9**
2.25	2	2	3		10	226.3	67	**29.6**	159.3	95	29.6	37.4	**135.3**	44	51	**20.5**	45	**19.9**
1.8	3.5	5	7		12	242.3	89	**36.7**	153.3	121	33.3	44.1	**171.8**	42	49	**18.5**	45	**18.6**
	5	6	3	1	11	215.0	66	**30.7**	149.0	157	42.2	51.3	**221.5**	40	45	**17.3**	22	**10.2**
0.8	12	2	1	2	3	392.8	171	**43.5**	221.8	520	57.0	70.1	**430.3**	53	58	**18.8**	64	**16.3**
0.2	11				10	217.7	81	**37.2**	136.7	442	67.0	76.4	**537.2**	42	48	**19.0**	53	**24.3**
2.1	10				8	227.1	78	**34.3**	149.1	704	75.6	82.5	**667.5**	46	48	**18.6**	64	**28.2**
0.4	10	1		2	7	239.9	56	**23.3**	183.9	269	52.9	59.4	**294.8**	43	47	**17.8**	92	**38.3**
2.7	8.5	1		1	5	318.2	73	**22.9**	245.2	378	54.3	60.7	**308.2**	46	47	**13.8**	110	**34.6**

indicators after the study by Kaiho (1994, 1999) and after the morphotype analysis of Rosoff and Corliss (1992). *Lenticulina* species, *Siphonina reticulata* and miliolids were considered oxyphylic after Kouwenhoven and Van der Zwaan (2004). Considering the species *Pullenia bulloides* and *Sphaeroidina bulloides* microhabitat or oxygen level preferences the picture is biased. According to Kaiho (1994, 1999), *Pullenia* spp. and *S. bulloides* are suboxic indicators, while Kouwenhoven and Van der Zwaan (2004) place them in the most oxyphylic "group 5". Regarding correlation with organic flux, Altenbach et al. (2003) associate the species *S. bulloides* with high organic carbon flux and content in sediment. Compilation of Den Dulk et al. (2000) classifies both species as shallow infaunal, and their spherical infaunal morphology (Rosoff and Corliss 1992) also supports the choice to include them among the infauna.

Stable isotope measurements

Regarding stable isotope analyses only the best-preserved foraminiferal shells were picked attempting to avoid any visible traces of recrystallization or infilling material under the light microscope. The presence of *Hoeglundina elegans* in some samples testifies for good preservation, as the species has an aragonitic test that is more susceptible to alter during diagenesis than calcite. Despite this, some stable oxygen isotope measurements from the lower part of the sequence were excluded (Tengelic-2 samples m, n, o, p, q, s, t1, t2, u and v, see values in brackets, Table 3) for having extremely negative $\delta^{18}O$ values not supported by faunal evidence. These samples were taken from more permeable sediments with higher silt content. However, the carbon isotope values of the same samples were found reliable because

Table 2 Counting results and calculations of core Tekeres-1. Inbenthic taxa are denoted by single asterisks, while oxyphylic taxa are denoted by double asterisks. The use of decimals is a result of counting broken tests or number of chambers making up a whole specimen. Calculated values plotted against depth in the core in Fig. 3 are typed in boldface

Tekeres-1 samples in core	Depth in core (m)	*Allomorphina trigonia* (REUSS)*	*Ammonia beccarii* (LINNÉ)	*Asterogerina planorbis* (D'ORBIGNY)	*Astrononion cf. italicum* (CUSHMAN & EDWARD	*Bolivina antiqua* (D'ORBIGNY)*	*Bolivina hebes* (MACFADYEN)	*Bolivina plicatella* (CUSHMAN)	*Bolivina reticulata* HANTKEN	*Bolivina scalprata var. miocenica* (MACFADYEN)	*B. spathulata* (WILLIAMSON) *f. spathulata**	*B. spathulata* (WILLIAMSON) *f. dilatata**	*Bolivina* spp.*	*Bulimina* sp 1*	*Bulimina elongata* (D'ORBIGNY)*	*Bulimina costata* (D'ORBIGNY)	*Cancris auriculus* (FICHTEL & MOLL)	*Cassidulina crassa* (D'ORBIGNY)	*Cassidulina oblonga* (REUSS)*	*Cassidulina subglobosa* (BRADY)*	*Cassidulina teretis* (TAPPAN)	*Cassidulina laevigata* (D'ORBIGNY)	*Ceratocancris haueriana* (D'ORBIGNY)	*Chilostomella* sp.*	*Cibicides lobatulus* (WALKER & JACOB)**	*Cibicides ungerianus* (D'ORBIGNY)**	*Cibicides* juveniles**	*Coryphostoma schmidi* (POPESCU)	*Dentalina* spp.	*Dentalina brevis* (D'ORBIGNY)	*Dentalina elegans* (D'ORBIGNY)	*Elphidium* sp.	*Epistominella species 1.*	*Epistominella species 2.*	*Fissurina* sp.	*Fursenkoina acuta* (D'ORBIGNY)*	*Gavelinopsis praegeri* (HERON-ALLEN & EARLA
A	47				3			2			8	26			12			2	3				3		61											16
B	55.4				3	1		1				1	1		35			34		2					10						1				3	1
C	71.25		30					2			9	1			71			6					1		13						2				27	3
D	77.05		3		2		3	4			2				14			3	13				6		27	1						1				6
E	86.15			2	3		7	1							4	29		3	6	2			6		9				1		8					2
F	94.6				3		3	1			2					5		1	2	6		2	1		8	6					1		1		1		
G	103.25				1			1			3				1	3			2	1			7		24	2				1	4		3				
H	111.5				1						2	1			27	18		5	30			3	5		14	3			1	1	1		2				
I	118													1	54	1			3				2		4						1		1				
J	135						22	6			3			1	2	1		5				5	17		7	1					16	1	2				1
K	143						4		1						42	37			5			1									1	1	3	1			
L	146.75				18		18		1						36	50			1	1			6		37	2			3		6		1	1	2		
M	154				5		39			2			2		30	46							6		6				7		8						
N	166.55			1	5		8	1		1	23	2	1		25	21			1	1		3	8		5			1	1.5		1		1		1		1
O	177.75		1	2	16		3	3		2	5				35	4			1	2			1		19				13					2	6	
P	182.25		3	4	18		11				6		2		27	1			2	1			2		20									1		
Q	191.25		5	3	3		8			1					31	2			3				2		9				2			1		1	5	
R	194.25		1			2	8			2	1	1			19	2			2	2			1		17				1						8	
S	198.25			1						1					32	2			4	20			2		8				2				4	2		
T	201.75			6	34		10		1	2					3	2			3	1		18	2		34							3	1		4	1	7
U	204.15				2		23			2	1				17	1			3	26			3		9				2		2		4				
V	207.25				20		1	1							29				1						14		8						15		3	1	1
W	211		5		10					2					37										4		2						19			9	4
X	217		6		15						16	1	1		34				1	1		1	1		9			1	3				1		1	4	
Y	222.25		1	2	17	2			3	9	1				14	2			12	44					36		4		2			1			2	2	5
Z	226			4	26		9		1	1				1	9				4	28			1		10	4	5	7				2			1	1	3
AI	230				17		6			5					11				5	10		1			13	4											14
BI	234	1			18	2	7			3				1	10	1			2	11			2		9	9		3				1					5
CI	238	1		3	15		8	1				2			0	13							7		15	5			1			1	3				11
DI	242	1		1	14		1	1	4		1	1	1		1	6			2			1	4		11		2	3	1				2		1		17
EI	245.5	3		1	9		2			3		5	1		0		1								13	30					14				2		5
FI	251	3		3	3		2		1						1	17							9		10	6			1		13	1			2		6
GI	255	1		2	10		11	1	1						2	3			6				10		13	4	2				9	1	1		1		6
HI	259	1			15			1		5					9	3			1				2		29						9	2					2
II	261	3		3	17				1		1	1	1		6	45			2				1	1	39							2			1		2
JI	265			4	15		3			2			1		12						2	1	4		38	5		1			4		5				2
KI	270.95				2	5	2		1			10			0	15							6		5	14		41				2		6	3		5
LI	273.1							1		3	20	4			41	2			3			4			5		4						1		2	15	
MI	276.25		8	2	3		4			1					17		1		2	1			6		5		1		2				1				

in permeable sediments the oxygen isotopes are more bound to travel by water than the carbon isotopes. The sample r with a relatively less negative $\delta^{18}O$ value (−3.2‰) compared to the rejected samples was kept and plotted in Fig. 4. Another problem was encountered while evaluating samples where $\delta^{13}C$ values measured in the benthic foraminiferal shells were found to be more positive, than in the planktonics. This is contrary to the expectations under normal marine conditions (see Anderson and Arthur 1983). Such samples were excluded from further calculations or plotting against core depth (Tengelic-2 u, Tekeres-1 MI, CI, X, W, V, U, E, C see values in brackets, Table 3). The sample EI in core Tekeres-1 was suspected to be diagenetically altered also based on its rather negative planktonic foraminiferal $\delta^{18}O$ value (−3.7‰) and close to identical $\delta^{13}C$ values in planktonic (1‰) and benthic foraminifera (0.8‰).

The measurements need a rather large quantity (~20 benthic and ~30 planktonic) of foraminiferal tests of the same species to avoid comparing values of different species with different vital effects. According to these requirements picking planktonic foraminifera monospecific was impossible, due to the lack of a persistent and abundant species, combined with the limited amount of rock samples from boreholes. Thus "bulk planktonic", a mixture of well-preserved planktonic

Table 2 (Contd.)

Tekeres-1 samples in core	Depth in core (m)	*Glandulina* sp.	*Globobulimina pyrula* (D'ORBIGNY)*	*Globulina* sp.	*Guttulina austriaca* (D'ORBIGNY)	*Guttlina communis* (D'ORBIGNY)	*Gyroidina umbonata* (SILVESTRI)	*Gyroidina parva* (CUSHMAN & RENZ)	*Gyroidina soldanii* (D'ORBIGNY)	*Hansawaia boueana* (D'ORBIGNY)	*Heterolepa dutemplei* (D'ORBIGNY)**	*Hoeglundina elegans* (D'ORBIGNY)	*Lagena* sp.	*Lenticulina calcar* (LINNÉ)**	*Lenticulina arcuata* (D'ORBIGNY)**	*Lenticulina* sp.**	*Melonis barleeanum* (WILLIAMSON)*	*Melonis pompilioides* (FICHTEL & MOLL)*	*Adelosina* sp.	*Quinqueloculina* sp.	*Miliolids***	*Spiroloculina* sp	*Nodosaria* spp.	*Nodosaria raphanistrum* (LINNÉ)	*Nonion commune* (D'ORBIGNY)	*Nonionella turgida* (WILLIAMSON)	*Oolina* sp.	*Oridorsalis umbonatus* (REUSS)	*Pullenia bulloides* (D'ORBIGNY)*	*Pullenia quinqueloba* (REUSS)*	*Reussella spinulosa* (REUSS)	*Siphonina reticulata* (CZJEK)**	*Sphaeroidina bulloides* (D'ORBIGNY)*	*Stilostomella adolphina* (D'ORBIGNY)	*Trifarina angulosa* (WILLIAMSON)	*Trifarina bradyi* (CUSHMAN)	*Uvigerina acuminata* (HOSIUS)*
A	47						7	6	11	13	42		3			1	2					2			3			2			1		2	32		
B	55.4						2			9	8					4	3	1				1			54			6								
C	71.25			2	1				3	1	21		1			1	3		1	3		1			33			10								
D	77.05		2				3		8		27	5	2	1		12					2	1	8.9	3	3			1						1		
E	86.15					3		2		8	27	5	2	1		12					2	1	8.9	3	3			1						1		
F	94.6	2				1		3			18	12	1	6		6					1	2	0.8		8			2			2			2	8	
G	103.25	2				2		7	6	12	6	2	6			10			1	2		2	2.7	2	4			7			1			6		
H	111.5	1			4	8		1	15	11		8				5						7	1	2	23			9								
I	118			2		12			3	107		3				2							0.2	3.5	14			3								
J	135			2	3	1		3	2	13		4				2				2		5	1	1	10			9			4					
K	143	1				2				142						1									12			3			1					
L	146.75					2		6	1	17	1	7				7	4	4		1		2	0.6					8		1				1		
M	154				1				1	4	1	3				2		5				5	1.1		5			2			2					
N	166.55					5		4	4	29		1				2				1		2	1.2	1	14			13		1	2			1		
O	177.75	12				5			7	10		6						3				1	2.6	1	2			42	1	1	1			23	1	
P	182.25	3				5		1	6	5		5				2		4				1	1.3	1	25		2	36				1		27	1	
Q	191.25					7			6	38		4						4					2.3		19		1	40			1			9	4	
R	194.25					2			1	85	2	2						2				1	0.4		6			28	1					12	1	
S	198.25					11			9	25		1	2			6						2	0.5		14			17						16	1	
T	201.75	3				9		1	9	8		2				2						4	4		6			4		2				2	4	
U	204.15					10		1	5	11						4		3					1		5	1		4	26					17		
V	207.25	2			8				2	18		4	1			3						1	1.5		37			35		1				4	2	
W	211	8				6			4	10		2										1			29			9						3		
X	217	4				5			1	2		3				1						1			33			27							4	
Y	222.25	4				3			3	5						4						2			23		1			1					2	
Z	226	1				14		1	20	9		1				3		2				1			21	11		2			2			1	5	
AI	230				4	2			5	3		2				2	1					1			21	3		3		4		1		3		
BI	234					8		1	14	15			2					8				1	0.2		6	4		1		1				3		
CI	238			1		9		4	7	26						3						1			3	2		29			2			1	1	
DI	242			1		12	1	1	7	31		2				1						1			16			24			2					
EI	245.5	1				2			2	31		2					2								14	3		23			2					
FI	251	1				8		1	6	25						5	3					1	0.4		21	3		14						2		
GI	255	5				4	4		5	13						1							0.8		45			5		1						
HI	259	2				11			7	28		3				1							3		3		1	2	18		3			2	3	
II	261	2				14	1		6	24						1						3			11			29		3	1			2		
JI	265			3		27			10	40		1				3	2					5	0.7			5		25		3				3	1	
KI	270.95			2		26		7		5		2	1			1	1				1	6	0.2		40	7		25		1	11			6	1	
LI	273.1	1							1	39		4					1	2				1	0.6	1	80			1								
MI	276.25	6				2		1	2	18						3		2					2		1			51						9	1	

taxa, was picked. Concerning the benthic, if monospecific picking failed, a related species was chosen for measurements. In borehole Tengelic-2 the two most common *Uvigerina* species, *U. semiornata* and *U. aculeata*, were picked for analyses. When both species (*U. semiornata* and *U. aculeata)* were measured in the same sample, surprisingly similar values were obtained. Unfortunately picking the same two species in Tekeres-1 in the required quantity failed, and other uvigerinids had to be selected for analyses (*Pappina bononiensis, U. macrocarinata)*, and if monospecific picking was not successful, mixed species of uvigerinids were picked in one sample. Except for *P. bononiensis* the values measured in the other three *Uvigerina* species were similar. Values of *P. bononiensis* were adjusted by adding $+1.6‰$ to compensate for the difference in the vital effect of the species, as calibrated from samples where it was possible to measure *U. macrocarinata* also (see description of these species in Báldi 1999, where *U. macrocarinata* is under the name *U. acuminata*).

Measurements were carried out on a VG SIRA 24 mass spectrometer (Utrecht State University) after foraminiferal tests were roasted in vacuum and treated with phosphoric acid at 100°C for 1.5 h. All isotope results are given in per mil relative to the Vienna Pee Dee Belemnite (VPDB) standard, generally referred to as "δ".

Results

Benthic foraminiferal distribution patterns

Counts of benthic foraminifera and calculations based upon benthic foraminiferal distribution patterns are

Table 2 (Contd.)

Tekeres-1 samples in core	Depth in core (m)	*Pappina bononiensis* (FORNASINI)*	*Uvigerina macrocarinata* (PAPP & TURNOVSKY)	*Uvigerina semiornata* (D'ORBIGNY)*	*Uvigerina cf. romaniaca* (PAPP & SCHMID)*	*Uvigerina undet.**	*Vaginulopsis pedum* (D'ORBIGNY)	*Valvulineria complanata* (D'ORBIGNY)*	Undetermined calcareous specimens	*Haplophragmoides* sp.	*Martinottiella communis* (D'ORBIGNY)	*Reophax* sp.	*Spiroplectammina carinata* (D'ORBIGNY)	*Sigmoilopsis* sp.	*Textularia* sp.	*Textularia mexicana?*	Undetermined agglutinated taxa	Total number of benthic	Number of inbenthic *	**Percentage of inbenthic taxa***	Corrected number of benthic	Number of planktonic foraminifera	Percentage of planktonic	Percentage of planktonic corrected for inbenthic	**Estimated paleowater depth (m)**	Counting listed taxa	Number of species including spp. and undet.	**Fisher's alpha diversity**	Number of oxyphyl taxa**	**Percentage of oxyphyl taxa****
A	47								5		0.5			2			4	274.5	57	**20.77**	217.5	10	3.5	4.4	**41.9**	28	29	**8.2**	104	**27.48**
B	55.4	9							4									227	62	**27.31**	165	8	3.4	4.6	**42.2**	21	21	**5.6**	66	**22.53**
C	71.25	1						4	3				18	4	1	2		306	121	**39.54**	185	47	13.3	20.3	**73.3**	26	27	**7.1**	21	**6.422**
D	77.05							4	1				51	1	6	5		229	46	**20.09**	183	110	32.4	37.5	**135.0**	31	31	**9.7**	50	**17.92**
E	86.15	1		8	9	10			6				37	6	2	12		254.9	41	**16.08**	213.9	297	53.8	58.1	**279.2**	39	39	**12.8**	51	**16.67**
F	94.6	1		5	5	10		5	5				43	11	5	9	6	222.8	48	**21.54**	174.8	396	64.0	69.4	**415.3**	42	44	**16.4**	47	**17.42**
G	103.25				14	16		5	1		0.4		29	11	4		1	215.1	51	**23.71**	164.1	300	58.2	64.6	**351.4**	40	40	**14.5**	55	**20.36**
H	111.5				10	3		11	2				9	1			1	248	94	**37.9**	154	322	56.5	67.6	**390.7**	36	36	**11.6**	33	**11.74**
I	118				4	3		2	3		0.4		4	1				234.1	70	**29.9**	164.1	311	57.1	65.5	**361.7**	25	26	**7.5**	113	**32.56**
J	135		6			3			5		0.2		34		1	2	1	204.2	24	**11.75**	180.2	373	64.6	67.4	**387.7**	38	42	**16.0**	27	**11.68**
K	143					1		1	4				18			4		286	53	**18.53**	233	297	50.9	56.0	**259.3**	22	23	**5.9**	144	**33.49**
L	146.75								4		0.2		9	2	8		1	269.8	54	**20.01**	215.8	405	60.0	65.2	**358.9**	36	39	**12.5**	63	**18.93**
M	154		2			1		1	4		1		43	5		1		241.1	43	**17.83**	198.1	331	57.9	62.6	**326.5**	30	32	**9.9**	14	**5.488**
N	166.55	6						1	2		1		28	1	4			236.7	73	**30.84**	163.7	172	42.1	51.2	**218.9**	43	44	**15.9**	38	**13.83**
O	177.75	1				1		4	5		0.3		40	2		5		291.9	113	**38.71**	178.9	256	46.7	58.9	**286.5**	40	45	**14.9**	30	**9.32**
P	182.25	2						9	7				16	1		2		261.3	93	**35.59**	168.3	238	47.7	58.6	**283.7**	36	39	**12.7**	27	**9.365**
Q	191.25							16	4				9	1		1		242.3	99	**40.86**	143.3	145	37.4	50.3	**211.8**	31	35	**11.2**	48	**16.53**
R	194.25							8	5				2	1		5	1	233.4	74	**31.71**	159.4	48	17.1	23.1	**81.2**	34	37	**12.4**	102	**30.41**
S	198.25	2						1	3				31	1		1		223.5	76	**34**	147.5	174	43.8	54.1	**242.4**	30	33	**10.7**	41	**15.5**
T	201.75							18	10				32	1		10		263	33	**12.55**	230	113	30.1	32.9	**114.8**	36	45	**15.6**	44	**14.33**
U	204.15	3				1			2				25	1				215	80	**37.21**	135	134	38.4	49.8	**208.2**	30	31	**9.9**	24	**10.04**
V	207.25	1						3	4				18			5		244.5	72	**29.45**	172.5	21	7.9	10.9	**52.6**	30	32	**9.8**	44	**15.25**
W	211	2						3					28	1		7		205	68	**33.17**	137	1	0.5	0.7	**36.8**	23	23	**6.6**	16	**7.24**
X	217	5						4			1.5		44			10		241.5	98	**40.58**	143.5	7	2.8	4.7	**42.3**	31	32	**9.9**	12	**4.734**
Y	222.25	1						6	3		0.2		22			6		245.2	86	**35.07**	159.2	47	16.1	22.8	**80.2**	34	36	**11.6**	49	**16.66**
Z	226	1				8		7	3				22	1		20	2	275	62	**22.55**	213	108	28.2	33.6	**117.6**	41	43	**14.3**	33	**10.71**
AI	230		15			16		6	5		1		12	1		7		204	68	**33.33**	136	60	22.7	30.6	**105.7**	32	35	**12.2**	22	**9.735**
BI	234		10			13		4	4		1			1		8	2	212.2	63	**29.69**	149.2	14	6.2	8.6	**48.6**	38	41	**15.1**	35	**14.16**
CI	238		19			23			7		0.2		12	1	3	2		247.2	74	**29.94**	173.2	227	47.9	56.7	**265.7**	37	41	**14.0**	51	**17.1**
DI	242		4			1	1				0.5		13	1			5	200.5	36	**17.96**	164.5	177	46.9	51.8	**223.5**	40	41	**15.6**	47	**18.99**
EI	245.5		12			7			9		0.5		0.5	1			7	207.5	54	**26.02**	153.5	146	41.3	48.7	**200.5**	31	34	**11.6**	76	**26.81**
FI	251						2		5		2		5	5		5		200.4	22	**10.98**	178.4	119	37.3	40.0	**147.3**	35	37	**13.3**	46	**18.67**
GI	255							4	6				33			2		212.8	23	**10.81**	189.8	118	35.7	38.3	**138.8**	32	36	**12.4**	33	**13.43**
HI	259							3	7				23	1	1			201	34	**16.92**	167	190	48.6	53.2	**234.8**	31	35	**12.3**	58	**22.39**
II	261							3	8	2			18	9	4	1	4	272	49	**18.01**	223	301	52.5	57.4	**272.5**	36	40	**12.9**	65	**19.29**
JI	265							9	6		2		4	2	1	4	6	261.7	49	**18.72**	212.7	212	44.8	49.9	**208.9**	37	44	**15.1**	86	**24.73**
KI	270.95							15	6	3	0.3	5	16	2	3	6	7	324.5	56	**17.26**	268.5	154	32.2	36.4	**129.9**	44	52	**17.5**	38	**10.48**
LI	273.1	40											7					283.6	128	**45.13**	155.6	92	24.5	37.2	**133.2**	26	27	**7.3**	48	**14.48**
MI	276.25	3						9	5		1		51	1		3	3	228	91	**39.91**	137	112	32.9	45.0	**175.5**	34	37	**12.5**	27	**10.59**

presented in Tables 1 and 2. From the counts the planktonic/benthic (P/B) ratio, the percentages of inbenthic and oxyphylic species and the Fisher's alpha diversity were calculated in each core and were plotted against core depth (Fig. 3).

Paleowater depth

The planktonic/benthic ratio was calculated as described in Van der Zwaan et al. (1990) to estimate paleowater depth. These paleowater depth results were previously published in Báldi et al. (2002), where they were used as an input for modelling basin subsidence.

The marine sequence of the Tengelic-2 borehole shows already an estimated paleowater depth of 300 m in the lowermost sample (w, 844 m) in marine silty clays overlying the terrigenous sediments. This lowermost sample contains species characteristic for neritic to bathyal depths (e.g. *Siphonina reticulata, Cibicides kullenbergi)*, as well as shallower elements (*Ammonia beccarii, Heterolepa dutemplei)*; thus transportation of the tests of these shallow living foraminifera cannot be excluded (Holcová, 1999). After rapid deepening the maximum upperbathyal paleowater depth of 600 m was reached (sample u). This planktonic/benthic ratio estimated upperbathyal paleowater depth is confirmed by the presence of neritic, bathyal species (e.g. *Siphonina reticulata,*

Cibicides kullenbergi) in the material. Until the top of NN 5 a gradual shallowing occurred to 100–150 m (833–802 m in core) comprising a rather significant relative sea-level drop. In the nannofossil zone NN 6, the paleowater depth remained 100–150 m except for a minor transient deepening to 300 m (Fig. 3, Table 1). Larger increases in paleowater depth based on foraminifera (e. g. about top of NN 5) coincide with peak abundances of calcareous nannofossil mentioned as indications of deeper environment by Nagymarosy (1982).

In Tekeres-1 the paleowater depth estimation shows some fluctuation in the lower part (278–205 m, samples MI-U). Steady deepening followed until 95 m; in this interval the sea reached a maximum depth of 400 m (sample F). A rather rapid sea-level drop of 350 m characterizes the top of NN 5 (samples F-C), which by NN 6 decreases to about 50 m of paleowater depth (Table 2, Fig. 3).

Paleoecology of benthic foraminifera

The percentage of the inbenthic foraminifera in the total benthic foraminifera assemblage was calculated to learn more about the trophic conditions. In the Early Badenian (NN 5), the percentage of inbenthic foraminifera was variable in both Tengelic-2 and Tekeres-1. By the end of the Late Badenian (NN 6) in the topmost sample (a) the number of inbenthic forms increased to a maximum of 52% in Tengelic-2 (Table 1, 2, Fig. 3).

Several carefully chosen strictly epibenthic species are used as indicators of bottom water oxygenation. The relative abundance (percentage) of these ''oxyphylic'' species in the total benthic fauna was calculated, intending to learn more about bottom water conditions. During NN 5 Badenian time in the Tengelic-2 borehole the percentage of the oxyphylic species amounted to over 20% in the total assemblage in the samples (w, v, u, t2), where the estimated paleowater depth reached its maximum. This shows that the percentage of oxyphilic taxa covaries with paleowater depth. However, in NN 6 Late Badenian times, the percentage of oxyphylic taxa shows a slightly decreasing trend independent of changes in the estimated paleowater depth (Table 1, Fig. 3). In core Tekeres-1 in NN 5 Badenian the percentage of oxyphylic taxa shows fluctuations regardless of paleowater depth, but the values are generally higher than in Late Badenian times (Table 2, Fig. 3).

In NN 5 Badenian time the Fisher's alpha diversity was found to be slightly higher (NN 5 average: 17.5) than in NN6 Late Badenian (NN 6 average: 14.1) based on the two studied cores. A clear, strong decreasing trend is observable throughout the Late Badenian NN 6 nannozone beginning at the NN 5/6 boundary in Tengelic-2 (Table 1, Fig. 3). The calculated Fisher's alpha diversities showed great variation in core Tekeres-1 during NN 5 Badenian.

Stable isotope trends

Core Tengelic-2

The measured oxygen isotope ratio (Table 3, Fig. 4) of the bulk planktonic decreases from $-1.6‰$ in the lowermost sample (w) to $-5‰$ in the topmost sample (a), equal to a negative shift of $-3.4‰$. At the same time the benthic oxygen isotope values exhibit an increasing trend. There is a negative shift of $-3‰$ from sample e to d, after which the increasing trend continues (samples d–a). Altogether the dominating increasing trend comprises a $+6‰$ positive shift from minimum (sample r) to maximum value (sample e).

The carbon isotope values of planktonic foraminifera show a strong negative shift from sample w to t2 in the lowermost part, followed by a continuous positive shift of about $+1.5‰$ up to the top of the studied Badenian interval. The benthic foraminiferal $\delta^{13}C$ values exhibit a positive shift of $1‰$ to a maximum (t1, s, r, q). Excluding the lowermost samples (w, v, t2) exhibiting some fluctuations, a very slow decreasing trend through the record becomes visible.

Core Tekeres-1

The Tekeres-1 planktonic $\delta^{18}O$ curve (averaging $-1‰$) can be divided into three parts (Table 4, Fig. 4). The lower part (278–205 m, samples LI-U) of the curve is strongly oscillating, while the middle part of the curve (205–95 m samples U-F) is rather stable. In the upper part (95–45 m samples F–A) there is a shift of $+1.7‰$ from 95 m to 71.3 m. The benthic $\delta^{18}O$ curve shows a similar pattern to the planktonic, but it is enriched by about $+1.5‰$ in the heavier isotope compared to values of the planktonic foraminifera.

The planktonic $\delta^{13}C$ in the lowermost interval (280–205 m, samples LI-U) fluctuates around $+1‰$, then displays a rather remarkable shift of $+1‰$ in the middle part from sample U to G, with a positive maximum of $+2‰$ at G (103.3 m). The upper part shows a decreasing trend. The benthic $\delta^{13}C$ values show a more or less similar pattern to the planktonic curve but are around $1‰$ more negative.

Oxygen and carbon stable isotope Δ δ values

Oxygen and carbon $\Delta\ \delta$ values equal the difference between Uvigerina and planktonic stable isotopes (Tables 3, 4):

$$\Delta\delta^{18}O = \delta^{18}O_{benthic} - \delta^{18}O_{planktonic},$$

$$\Delta\delta^{13}C = \delta^{13}C_{benthic} - \delta^{13}C_{planktonic}.$$

These values were plotted against core depth to follow changes of the isotopic gradient of the water column through the record (Fig. 4).

In core Tengelic-2 (Table 3, Fig. 4), the $\Delta\ \delta^{18}$ O values show an increase of about +6‰ from slightly negative values at the bottom to 6‰ at the top. This positive shift is especially clear in the upper part of the core (samples a-d) corresponding to the topmost NN 6 believed to be the Bolivina-Bulimina zone. The $\Delta\ \delta^{13}$ C record shows a slight, but clear, decreasing trend towards lower values through the Badenian time period (samples s to a), except for the lowermost part (samples w, v) . This tendency comprises a shift of −1.5‰ (from sample u to a).

In core Tekeres-1 (Table 4, Fig. 4), the $\Delta\ \delta^{18}$ O results show an increasing trend (e.g. +1‰ from sample P to H) with some fluctuation in the lower parts of the record. The $\Delta\ \delta^{13}$ C record is rather fluctuating in general. The middle part (sample P to G) of the record is dominated by a negative shift of around −2‰, reaching the minimum value of the record in sample G. In the upper part of the core there is a positive shift from sample G to A.

Discussion

Interpretation of benthic foraminiferal distribution

Paleobathymetry

The most prominent feature of the paleobathymetric curve is a significant sea-level drop attributed to uplift at the end of NN 5 nannoplankton zone (see details in Báldi et al. 2002). This tectonic movement has played an important role shaping the Badenian landscape, separating the previously connected Central Paratethys Basins from the Eastern Paratethys (Rögl 1998b). This event may have triggered the mid Badenian evaporite formation in the Carpathian Foredeep and the Transylvanian Basin (see further discussion Sect. "The mid Badenian salinity crisis").

During the NN 5 nannozone the Paratethys in the Pannonian Basin was known to reach at least bathyal depths (Báldi 1997; Báldi et al. 2002). The bathyal depth estimation based on planktonic/benthic ratios is confirmed by the presence of species characteristic for greater (neritic to bathyal) depths (e.g. *Siphonina reticulata, Cibicides kullenbergi)*. The NN6 Badenian sediments in the studied cores were deposited at much shallower depths (mostly < 200 m, see paleowater depth curve in Fig. 3) based on planktonic/benthic ratios. This shallowing with the rather abrupt sea-level drop at the end of NN 5 as is expected determines the benthic foraminiferal assemblages in many ways (Fig. 3). However, the trends observable during NN 6 Late Badenian cannot be explained exclusively by changes of paleowater depth, as it was rather stable in this time interval. The percentage of species with known ecologic needs, inbenthic or oxyphylic taxa and benthic foraminiferal diversity show changes (Figs. 3, 5b) more plausible to explain in terms of oxygen and food availability.

Benthic foraminifera paleoecology

In the present study environmental changes controlling the in-sediment depth distribution of benthic foraminifera were assessed. According to the TROX model the two limiting factors, oxygen content and organic matter, serving as food resources determine the in-sediment depth distribution of benthic foraminifera (Jorissen et al. 1995). An intricate interplay exists between the oxygenation of bottom water and organic matter content of sediment. By common sense degradation of organic matter in excess amount at the sea bottom depletes water in oxygen. However, these two factors, oxygen and food, both crucial to benthic life are to be discussed separately here.

The percentages of inbenthic and oxyphylic taxa in the total counts of benthic foraminifera were used as indicators of these two parameters. The percentage of inbenthic taxa reflecting food availability and the percentage of oxyphylic taxa reflecting oxygenation of bottom water showed characteristic changes by Late Badenian time. While in the Early Badenian the organic matter content, meaning food for benthics, was rather variable, it most likely never reached a level of hampering oxygenation of the bottom waters. However, by Late Badenian times the number of inbenthic forms doubled, indicating that organic matter arrived at the sea floor in excess amount, using up oxygen and causing a significant decrease of oxyphylic species. In addition, increasing stratification of the water column (see Sect. "Oxygen and carbon stable isotope $\Delta\ \delta$ values") indicated by the oxygen isotopes ($\Delta\ \delta^{18}$ O) caused extra oxygen depletion at the sea bottom. The decreasing amount of oxygen meant stress for the benthic community, and thus the diversity of benthic foraminifera declined (Figs. 3, 5b).

Evaluation of stable isotope trends

The measured oxygen and carbon isotope values of both cores were averaged for the NN 5 Early and mid Badenian and the NN 6 Late Badenian period of time to ease further discussion (Table 3, 4):

The δ^{18}O values measured in *Uvigerina semiornata* and *U. aculeata* from the same samples showed minimum differences in Tengelic-2 (Table 3). This can be most likely attributed to the fact that these species are taxonomically closely related (Van der Zwaan et al. 1986). In Tekeres-1 (Table 4), where different uvigerinid species were chosen for analyses, the results were slightly more scattered depending on which species was measured (Fig. 4). In agreement with this observation the *Pappina bononiensis* values had to be compensated for vital effects in respect to all the other *Uvigerina* species. Additionally, *P. bononiensis* synonymous to *Uvigerina bononiensis* is not a member of the " *semiornata*-group" like the rest of the species used for measurements in the present work (Van der Zwaan et al. 1986). This

Table 3 Stable isotope results ($\delta^{18}O$, $\delta^{13}C$) of core Tengelic-2. Values plotted against depth in the core in Fig. 4 are typed in boldface

Tengelic-2 samples	Depth in core	δO^{18} planktonic (‰)	δC^{13} planktonic (‰)	δO^{18} *U.semiornata* (‰)	δC^{13} *U.semiornata* (‰)	δO^{18} *U.aculeata* (‰)	δC^{13} *U.aculeata* (‰)	δO^{18} average benthic(‰)	δC^{13} average benthic(‰)	$\Delta O^{18} = \delta O^{18}_{\text{benthic}} - \delta O^{18}_{\text{planktonic}}$	$\Delta C^{13} = \delta C^{13}_{\text{benthic}} - \delta C^{13}_{\text{planktonic}}$
a	738.45	**−5**	**2**	1.5	0.2			**1.5**	**0.2**	**6.5**	**−1.8**
b	743.8	**−3.7**	**1.5**	0.5	0.2			**0.5**	**0.2**	**4.2**	**−1.3**
c	749	**−3.4**	**1.4**	0	0.3			**0**	**0.3**	**3.4**	**−1.1**
d	754.05	**−4.6**	**1.9**	−1.7	0.6			**−1.7**	**0.6**	**2.9**	**−1.3**
e	759.9			1.5	0.2	1.6	0.3	**1.55**	**0.25**		
f	764.5			1.5	0.3	0.9	0.3	**1.2**	**0.3**		
g	768.85	**−1.8**	**1.8**			0	0.1	**0**	**0.1**	**1.8**	**−1.7**
h	773.75			−0.8	0.3			**−0.8**	**0.3**		
ij	777.85	**−2.9**	**1.6**	0.8	0.3			**0.8**	**0.3**	**3.7**	**−1.3**
k	781.45	**−2.7**	**1.8**	−0.9	0.5			**−0.9**	**0.5**	**1.8**	**−1.3**
l	785.55	**−3.3**	**2**	0.2	0.3			**0.2**	**0.3**	**3.5**	**−1.7**
m	789.5	(−7)	**1.4**	−0.9	0.3				**0.3**		**−1.1**
n	793	(−6.9)	**1.2**	−3.5	0.5				**0.5**		**−0.7**
o	796.5	(−6.2)	**1.7**	−1.8	0.3				**0.3**		**−1.4**
p	801.3	(−6.9)	**1.4**	−3.3	0.3				**0.3**		**−1.1**
q	807.05	(−8.2)	**0.9**	−2.7	0.5				**0.5**		**−0.4**
r	812.75	**−3.2**	**1.2**	−4.3	0.6			**−4.3**	**0.6**	**−1.1**	**−0.6**
s	817.8	(−7.1)	**0.9**		0.6				**0.6**		**−0.3**
t1	823.4	(−8.9)	**1**	(−5.6)	0.6	(−5.5)	0.7		**0.65**		**−0.35**
t2	828.75	(−9.7)	**0.6**			(−4.9)	0.1		**0.1**		**−0.5**
u	833.35	(−7.95)	**0.35**		0.4				**0.4**		**0.05**
v	838.35	(−6)	**1.1**				0		**0**		**−1.1**
w	844	**−1.6**	**2.4**			−2.2	0	**−2.2**	**0**	**−0.6**	**−2.4**

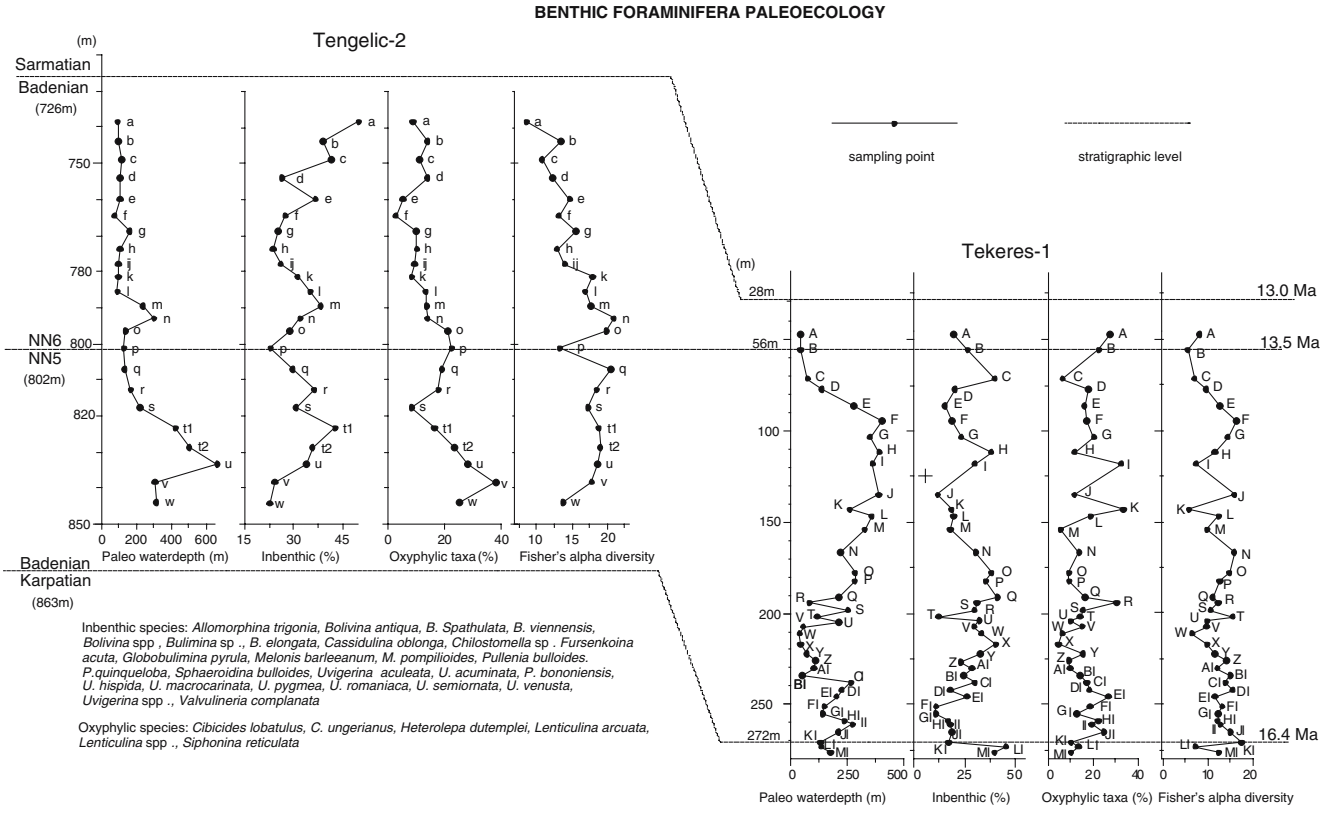

Fig. 3 Benthic foraminiferal results of the two studied boreholes Tengelic-2 (Table 1) and Tekeres-1 (Table 2) plotted against depth in the core. From left to right the benthic foraminiferal ecology: *1*. Paleowater depth estimation based on corrected planktonic/benthic ratio of foraminifera (calculations after Van der Zwaan et al. 1990, also in Báldi et al. 2002). *2*. The percentage of inbenthic taxa in the total number of benthic foraminifera. *3*. The percentage of oxyphylic taxa in the total number of benthic foraminifera. *4*. Fisher's alpha diversity is calculated using the formula given by Fisher et al. (1943) with the constants from Williams (1964, Fig. 125)

taxonomic difference is expressed on the generic level by Rögl (1998a) who designated it to the genus *Pappina*. It seems reasonable to suppose that the degree of scatter of the two different uvigerinid species depended on their taxonomic distance.

Oxygen isotopes

δ^{18}O in most samples corresponds well to a normal marine average (Zachos et al. 2001) supported by the benthic foraminiferal evidence presented here (Table 1, and see averages above) contributing to the credibility of the measurements. This is in accordance with the well-known fact that the Badenian is the last fully marine time period in the history of the Central Paratethys (e.g. Rögl 1998a).

The oxygen $\Delta\ \delta$ reflects density stratification of the water column (Tables 3, 4; Fig. 4). The $\Delta\ \delta$ oxygen isotope averages for NN5 Badenian (1.36‰) and Late Badenian NN 6 (3.22‰) were found comparable to World Ocean averages as mentioned for the Early (1.75‰) and Middle-Late Miocene (2.25‰) by Kennett (1985). However, we have to keep in mind that the World Ocean was deeper than the Central Paratethys, thus finding larger $\Delta\ \delta^{18}$ O in NN 6 Central Paratethys (3.22‰) than in the World Ocean (2.25‰) points to very strong stratification in the case of an inland sea of about 200 m paleowater depth at the time.

The $\Delta\ \delta$ oxygen values show a strong positive shift (1–1.5‰ based on averages), especially pronounced in the Late Badenian. This trend undoubtedly indicates increasing vertical stratification of the water column (Figs. 4, 5b). The decreasing trend observed in planktonic oxygen isotopes and the increasing trend in benthic combined, results the increasing trend of $\Delta\ \delta^{18}$ O values (Fig. 4). Isotope studies of Gonera et al. (2000) from the Carpathian Foredeep, showing increasing difference of planktonic and benthic oxygen values with time, support the regional character of this trend. Therefore it is reasonable to believe that the increasing stratification of the water column was not just a local phenomenon of the studied southern Pannonian Basin, but that it also affected the whole Central Paratethys, where the basins were deep enough and no other factors (e. g. tectonics) overprinted the signal.

Gonera et al. (2000) interpreted the Forecarpathian oxygen isotope record by using transfer functions (Moore et al. 1981; Erez and Luz 1983), estimating the actual temperature of surface and bottom waters. Such

Table 4 Stable isotope results ($\delta^{18}O$, $\delta^{13}C$) of core Tekeres-1. Values plotted against depth in the core in Fig. 4 are typed in boldface

Tekeres-1 samples	Depth in core	δO^{18} plank-tonic (‰)	δC^{13} plank-tonic (‰)	δO^{18} *U.semi-ornata* (‰)	δC^{13} *U.semi-ornata* (‰)	δO^{18} *U.acul-eata* (‰)	δC^{13} *U.acul-eata* (‰)	δO^{18} *P.bonon-iensis* (‰)	δC^{13} *P.bonon-iensis* (‰)*	δO^{18} *U.macro-carinata* (‰)	δC^{13} *U.macro-carinata* (‰)	δO^{18} *Uvigerina* spp. (‰)	δC^{13} *Uvigerina* spp. (‰)	δO^{18} average benthic (‰)	δC^{13} average benthic (‰)	$\Delta O^{18} = \delta O^{18}_{\text{benthic}} - \delta O^{18}_{\text{planktonic}}$	$\Delta C^{13} = \delta C^{13}_{\text{benthic}} - \delta C^{13}_{\text{planktonic}}$
A	47	**0**	**0.4**	1.8	0.2									**1.8**	**0.2**	**1.8**	**−0.2**
B	55.4	**−0.8**	**1.3**					1	0.7					**1**	**0.7**	**1.8**	**−0.6**
C	71.25	(0.7)	(0.6)					(1.8)	(1.2)								
D	77.05	**−0.2**	**1.3**														
E	86.15	(−1.1)	(0.5)	(0.3)	(0.7)	(0.4)	(0.4)										
F	94.6	**−1.5**	**1.5**	0.4	0.8	0.5	0.4							**0.45**	**0.6**	**1.95**	**−0.9**
G	103.25	**−1.5**	**2.3**			0.5	0.4							**0.5**	**0.4**	**2**	**−1.9**
H	111.5	**−1.3**	**1.9**			0.8	0.6							**0.8**	**0.6**	**2.1**	**−1.3**
I	118	**−1.1**	**1.9**			1	0.7							**1**	**0.7**	**2.1**	**−1.2**
J	135	**−1**	**1.8**			0.8	0.7			0.7	0.9			**0.75**	**0.8**	**1.75**	**−1**
K	143	**−0.7**	**1.1**									0.8	0.4	**0.8**	**0.4**	**1.5**	**−0.7**
L	146.75	**−1.3**	**1.3**														
M	154	**−1.2**	**1.1**							0.3	0.2			**0.3**	**0.2**	**1.5**	**−0.9**
N	166.55	**−1.3**	**0.7**					0.5	−0.3	0.2	0.1			**0.35**	**−0.1**	**1.65**	**−0.8**
O	177.75	**−0.8**	**0.9**					0.4	0.6	0.4	0.2			**0.4**	**0.4**	**1.2**	**−0.5**
P	182.25	**−1.1**	**0.9**					0.1	0.7					**0.1**	**0.7**	**1.2**	**−0.2**
Q	191.25																
R	194.25																
S	198.25																
T	201.75																
U	204.15	**−2.3**	**0.6**					−0.6	0.1					**−0.6**	**0.1**	**1.7**	**−0.5**
V	207.25	(−0.1)	(0)					(0.2)	(0.9)								
W	211	(−0.3)	(0.4)					(0.2)	(0.4)								
X	217	(−0.7)	(0.8)					(0)	(1.4)								
Y	222.25	**−1.8**	**1.7**														
Z	226	**−1.4**	**1.5**							−0.2	0.4			**−0.2**	**0.4**	**1.2**	**−1.1**
AI	230	**−1.1**	**0.9**							0.1	0.4			**0.1**	**0.4**	**1.2**	**−0.5**
BI	234																
CI	238	(0.1)	(0)							(0.1)	(0.7)						
DI	242	**−0.6**	**1.1**							1.2	0.8			**1.2**	**0.8**	**1.8**	**−0.3**
EI	245.5	(−3,7)	(−1)							(−0,2)	(−0,8)						
FI	251		**1**														
GI	255	**−0.6**	**1**														
HI	259	**−1.3**	**1.3**														
II	261	**−2.5**	**1**														
JI	265	**−0.9**	**1.7**														
LI	273.1	**−0.5**	**1**					0.5	0.3					**0.5**	**0.3**	**1**	**−0.7**
MI	276.25	(−0.8)	(0.4)					(0.3)	(0.6)								

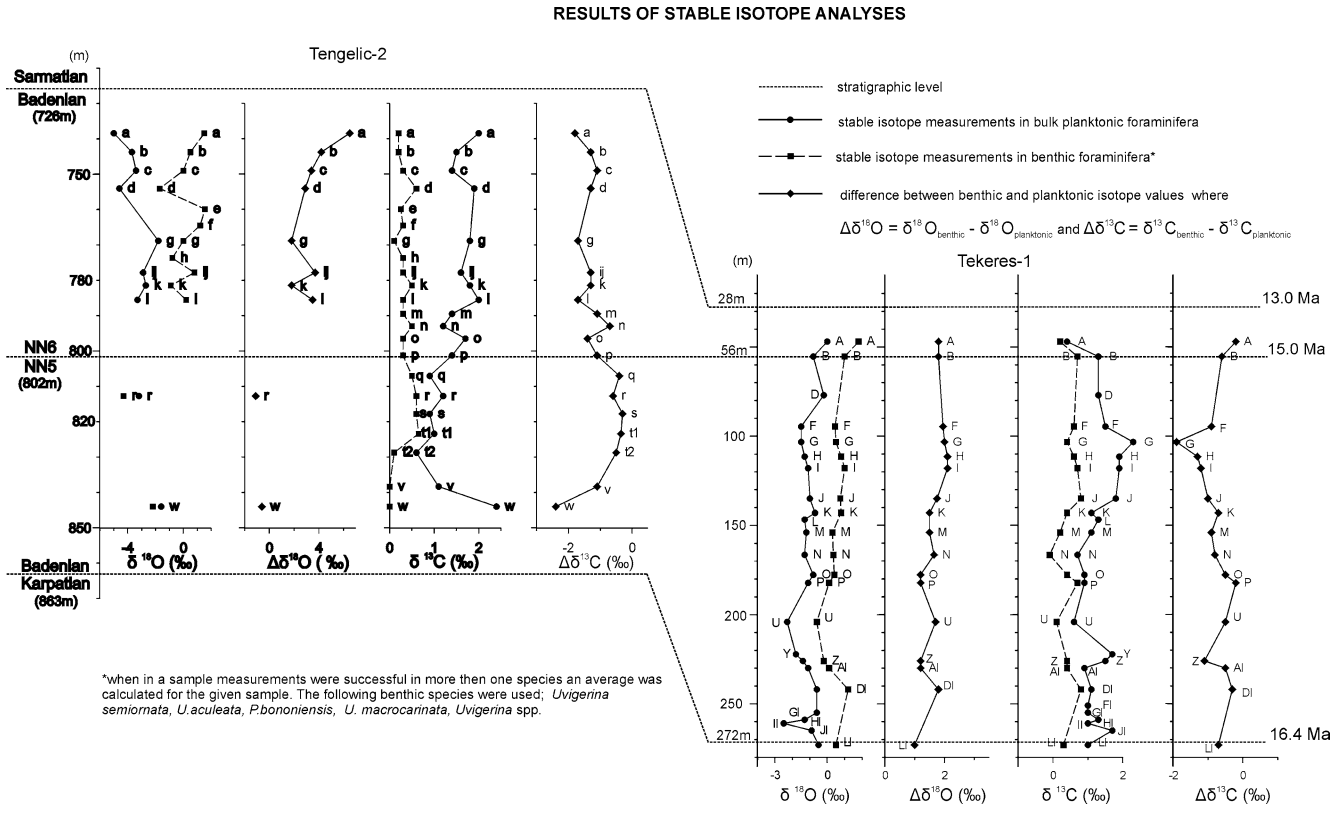

Fig. 4 Results of stable isotope analyses of the two studied boreholes Tengelic-2 (Table 3) and Tekeres-1 (Table 4) given in per mil (‰) relative to the Vienna Pee Dee Belemnite (VPDB) standard. From left to right *1*: Oxygen isotope (δ^{18}O) values of bulk planktonic (*dot*) and benthic uvigerinids (*square*) *2*. Difference ($\Delta\ \delta^{18}$ O) between uvigerinids (benthic) and planktonic oxygen isotope values ($\Delta\ \delta^{18}\ O = \delta^{18}O_{benthic} - \delta^{18}O_{planktonic}$) 3. Carbon isotope ($\delta^{13}$C) values of bulk planktonic (*dot*) and uvigerinids (*square*) 4. Difference ($\Delta\ \delta^{13}$ C) between uvigerinids and planktonic carbon isotope values ($\Delta\ \delta^{13}\ C = \delta^{13}C_{benthic} - \delta^{13}C_{planktonic}$)

calculations are based on the premise that temperature is the main control on the variation of oxygen isotope values. However, here a more cautious approach was followed by taking into account that in the case of an inland sea the isotope values greatly depend on factors unknown to an open ocean environment. In the case of a rather limited water body of an inland sea isotope values greatly depend on the δ^{18}O and δ^{13}C of riverine inflow, besides evaporation. Oxygen isotope values of runoff water can show great variation depending on the source area (e.g. Swart et al. 2001) and the limits of using isotope data for salinity reconstructions have been shown by Mátyás et al. (1996) for the Pannonian Basin. The Late Badenian strongly negative δ^{18}O values (average −2.82‰) measured in planktonic foraminifera is preferably interpreted as not only cooler, but also more importantly less saline surface water.

Carbon isotopes

The benthic carbon isotope values, averaging 0.43‰ for NN 5 and 0.33‰ for NN 6, are comparable to the World Ocean deep water record of Zachos et al. (2001) (around 1.6–1.8‰) of the studied interval. However, while the World Ocean record exhibits a positive shift in benthic δ^{13}C in the studied time interval, the presented Paratethys records show a weak negative shift. This weak negative trend, especially observable in the NN 6 part of the benthic δ^{13}C curve (Fig. 4), is probably related to enhanced benthic eutrophication.

The slight decrease of benthic carbon isotope values is coupled with a more clearly expressed increasing trend of the planktonic δ^{13}C values and results in a decrease of the $\Delta\ \delta^{13}$ C. These trends are probably related to primary production creating isotopically light marine organic matter in the photic zone sinking to the sea floor, thus depleting surface waters and enriching bottom waters in the lighter isotope (Fig. 4). This sign of increasing eutrophication through Badenian times is especially pronounced in the Late Badenian.

Circulation and climate

It is generally known that oceanic circulation influences the climate of the surrounding land. A well-known example of this is the Gulf-current making North Western Europe's climate more temperate by transporting heat to higher latitudes. However, it is also true that the climate determines oceanic circulation. In an inland sea

connected with the open ocean two sorts of circulation can develop depending on the balance of the fresh-water inflow (precipitation and runoff), versus evaporation, if we suppose an unrestricted exchange of water masses through a deep enough strait.

If evaporation exceeds the net fresh water and oceanic inflow an *antiestuarine circulation* develops in an inland sea. This involves a surface inflow of normal salinity water from the World Ocean into the inland sea. This inflowing water becomes more saline due to evaporation, sinks and flows out of the inland sea as a more saline deeper-water mass. In the case of such a circulation system the mass balance is positive with respect to salinity. The water column will not to be much stratified due to downwelling of more saline, heavier water. The reduction or absence of density stratification contributes to a well-ventilated bottom. This circulation type has a positive salt balance that makes the accumulation of evaporites possible. A warm, dry climate favours an antiestuarine type of circulation where evaporation exceeds the effect of inflow from rivers and the ocean, in addition to precipitation. The Mediterranean Sea (Miller 1983) and the Red Sea (Ross 1983) among other present day seas have an antiestuarine circulation.

An *estuarine circulation* evolves if the net inflow of fresh water exceeds evaporation, thus a less saline surface water layer is formed. This water on the surface flows from the continent towards the ocean, while normal saline deep water enters from the open ocean. The salt balance of the sub-basin is negative compared to the ocean, due to dilution by freshwater, so the sub-basin becomes hyposaline as a consequence. If hyposaline water originating from runoff or precipitation piles up on top of normal saline water over the whole basin then we might expect a strong, shallow picnocline, possibly hampering vertical circulation. In the case of estuarine circulation dysoxic or anoxic conditions can develop at the bottom. The present day example of the Sea of Marmara or the Black Sea can be regarded as an analogue.

Early Badenian (NN5) circulation

A simple two-layer circulation model was developed for the Paratethys. A prerequisite is that the connecting corridors should be sufficiently deep to allow two-way circulation. During the Early Badenian a deep strait connected the Central Paratethys to the Mediterranean (Daniels and Ritzkowski 1970; Rögl et al. 1978; Steininger and Rögl 1984; Rögl 1998b).

The proposed circulation model for Early and mid Badenian times involves a surface water inflow of normal marine water from the Mediterranean into the Paratethys. In return, more saline, Paratethyan deep water downwells and flows back to the Mediterranean. This *antiestuarine* model implies that the net evaporation is increasing towards the continent, to the northeast. According to this model heat is transported by the

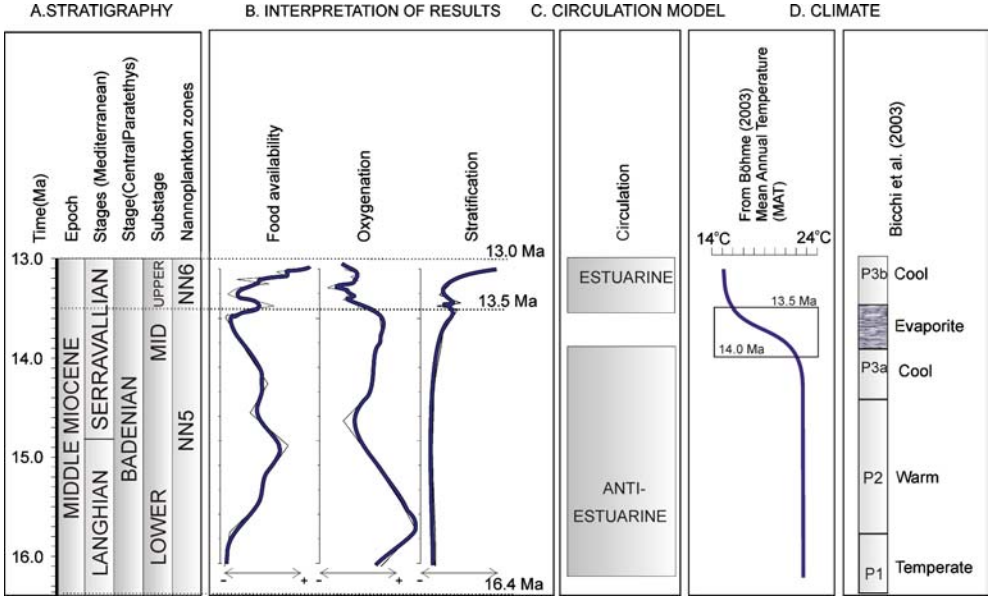

Fig. 5 Interpretation of results and the circulation model in the light of climate reconstructions of Böhme (2003) and Bicchi et al. (2003). **a** Stratigraphic frame used to correlate the presented core. The Paratethys stage Badenian correlated to global scales and dated after Rögl (1998a), absolute age of NN 5/6 boundary are based on Berggren et al. (1995). **b** Interpretation of results regarding environmental parameters controlling benthic foraminiferal distribution: *1*. Food availability based on inbenthic foraminifera. *2*. Oxygenation of bottom water based on the oxyphylic taxa. *3*. Stratification of the water column reconstructed from the $\Delta\ \delta^{18}$ O curve. **c** Tentative circulation model of the Central Paratethys. **d** Climate reconstruction of Böhme (2003) based on vertebrates. The rapid cooling period is marked by a rectangle. The climate reconstruction given by Bicchi et al. (2003) based on planktonic foraminifera of the Carpathian Foredeep is also presented

surface current from the lower latitude Mediterranean to the Central Paratethys (Figs. 5c, 6).

The first part of the NN 5 Badenian (16.4–15 Ma) is a period of time globally known to have a remarkably warm climate referred to as the Mid-Miocene Climatic Optimum (17–15 Ma, Zachos et al., 2001, among others). Evidences of this global climatic optimum in the Central Paratethys area are presented in many recent publications (Schwarz 1997; Gonera et al. 2000; Ivanov et al. 2002; Böhme 2003; Bicchi et al. 2003, Fig. 5d). From Early Badenian times, diverse coral reefs with their equally diverse crustacean faunas (Müller 1984, 1996) are well-known in the Central Paratethys from shallow-water formations. Occurrence at such high latitudes of reef building corals with high diversity associated fauna is exceptional (Pál Müller 1996, personal communication). The Early Badenian foraminiferal assemblages show relatively high diversity also (Fig. 3). Similarly the occurrence of deep weathering with lateritic bauxite at the high paleolatitude of 45°N in Germany shows extremely warm climatic conditions during the early Middle Miocene (Schwarz 1997). Besides being the result of the global climatic optimum, the exceptionally warm climate of the region is probably in part the result of heat transport in an antiestuarine setting, where the surface water current from the lower latitude

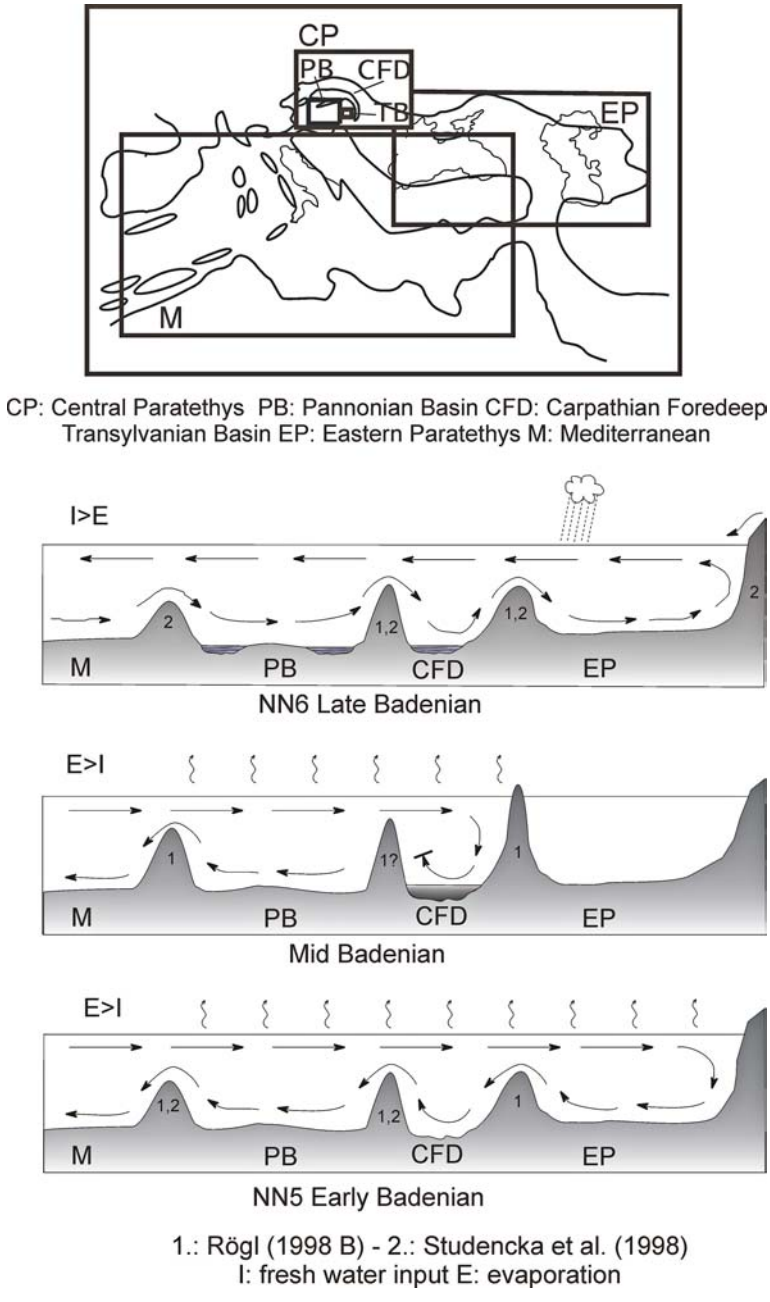

Fig. 6 Schematic representation of the marine Badenian sedimentary basins showing a two-layered circulation model. **a**. Early Badenian (NN 5) antiestuarine circulation. **b**. Mid Badenian salinity crisis where antiestuarine circulation is considered and shallow sill depth restricts deep water outflow to the Central Paratethys. *Dark colours* indicate evaporitic sediments and brine at the bottoms of deeper basins like the Carpathian Foredeep. *c* Late Badenian NN 6 estuarine circulation is suggested. *Dark colours* indicate organic-rich sediments accumulating at the bottom of deep basins in accordance with the model presented here. Seaways connecting waterbodies are taken from paleogeographic maps of Rögl (1998b) and Studencka et al. (1998) denoted by numbers 1 and 2, respectively. If opinions diverge (Rögl 1998b; Studencka et al. 1998), only the version used in the figure is denoted

Mediterranean takes warm water into the Central Paratethys (Figs. 5, 6).

It is a generally accepted view for the Early Badenian Paratethys to have a fauna similar to the Mediterranean (Rögl et al. 1978). The benthic foraminiferal fauna studied here is a slightly impoverished Mediterranean fauna in general. Other marine fossils show the same affinity to the Mediterranean (Rögl et al. 1978). As most marine organisms have a planktonic life stage and even benthic foraminifera lacking such life stage has been found in the plankton net (John 1987), possibly these organisms used the surface currents from the Mediterranean for spreading towards the Paratethys.

The mid Badenian salinity crisis

The paleobathymetric curve shows a major sea-level drop at the end of the NN 5 nannofossil zone, related to uplift as shown by Báldi et al. (2002). This tectonic movement is believed to separate the previously connected Central Paratethys Basins from the Eastern Paratethys (Rögl 1998b). This tectonic event might have triggered the formation of widespread evaporitic layers in the Carpathian Foredeep and the Transylvanian Basin by mid Badenian time (Rögl 1998b). Climate also plays an important role in processes leading to evaporite formation. Tectonic events can change the corridors connecting water bodies, restricting the inflow to a level where evaporation can exceed the fresh water input. Evaporation on the other hand is climate controlled, and thus the higher temperatures of the Mid-Miocene Climatic Optimum could have created favourable conditions for evaporite formation (Fig. 5). According to Zachos et al. (2001), these warm temperatures lasted 17–15 Ma followed by a decline at 15–14 Ma, while in continental deposits of mid-latitude Europe the cooling was delayed. According to Böhme (2003) the climatic optimum had lasted until 14 Ma followed by a rapid cooling period at 14–13.5 Ma. This delayed cooling of Europe reconstructed by Böhme (2003) could be the result of heat transport of an antiestuarine circulation system. Thus, with regard to the uncertainties in the stratigraphic resolution, this lasting climate maximum could have contributed to the formation of evaporites. The exact stratigraphic position of the negligibly short (0.2 Ma in Balintoni and Petrescu 2002) duration of the evaporite event cannot be identified in the foraminifera and isotope record presented here, but evaporite formation is certain to happen under antiestuarine circulation. An antiestuarine circulation model alone implies the positive salt-balance necessary for the formation of evaporites, where net evaporation increases towards the continent. According to several reconstructions the Central Paratethys was not connected to the East Paratethys in mid Badenian (e.g. Rögl 1998b), thus making the Carpathian Foredeep and the Transylvanian Basin the easternmost part of the Central Paratethys, a likely scene for evaporite formation. Balintoni and Petrescu (2002) also describe this type of circulation, considering a deep water brine formation as suggested by the present model (Fig. 6). However, their model supposes a surface current as input with already brackish water (Gontsharova 2001) from the Eastern Paratethys through a corridor connecting the Eastern Paratethys with the Carpathian Foredeep and the Transylvanian Basin (Studencka et al. 1998). This brackish water is the inflow to evaporate making possible the formation of salt deposits. The main argument supporting an Eastern Paratethys connection is the absence of evaporites in the Pannonian Basin, thus excluding the possibility of a connection between the evaporitic basins and the Pannonian Basin (Balintoni and Petrescu 2002). Here the idea of a one-way restricted circulation between Pannonian Basin and the Carpathian Foredeep is introduced, where the sill-depth does not allow the outflow of the saline brine from the Carpathian Foredeep to the Pannonian Basin explaining the absence of evaporites in the latter. Such circulation pattern, on the other hand, allows normal marine surface water to flow from the Pannonian Basin to the Carpathian Foredeep through the Transylvanian Basin (Fig. 6).

The Late Badenian (NN6)

The proposed circulation model for the Late Badenian (NN 6 to Badenian/Sarmatian boundary) period of time is *estuarine*. In this model Eastern Paratethys surface water enriched in the lighter oxygen isotope due to mixing with low value runoff and precipitation flows into the Central Paratethys, while isotopically heavier Central Paratethys deep water enters the East Paratethys in return. Such a circulation was suggested by Kókay (1985), based on hyposaline and normal saline mollusc faunas at sites very close to each other, in the absence of tectonic features between the two areas. The rather negative oxygen isotope average values of −2.82‰ reconstructed for the Late Badenian surface water are rather low compared to a normal marine average. This supports a strong *estuarine* type of circulation confirming Kókay's (1985) idea of a Late Badenian "Konkian" estuarine circulation. The increasing $\Delta\ \delta^{18}$ O values through Badenian times reaching a maximum by Late Badenian with corroborating foraminiferal evidence indicates that increasing stratification of the water column also points to an estuarine type of circulation (increasing inbenthic, decreasing oxyphylic percentages, declining diversity).

The high $\Delta\ \delta^{18}$ O values reached by the end of NN 6 Late Badenian are the result of isotopically very negative planktonic δ^{18}O values (e. g. Tengelic-2 samples a–d averaging about −4‰, Fig. 4). Gonera et al. (2000) observed a similar post-evaporite isotope trend which was interpreted in terms of temperature changes reflecting climate. It is obvious that the cooling trend of the Mid-Miocene affected the Paratethys also (Ivanov et al. 2002 among others) by lowering the surface water δ^{18}O values.

However, it cannot be excluded that the slightly reduced salinity especially at the end of NN 6 Badenian, correlating to the *Bulimina-Bolivina* Zone and the "Konkian" facies of Kókay (1985), could have contributed to the low isotope values also. Furthermore, it makes sense to interpret it as a prelude to the following Sarmatian times, when oligohaline shallow-water fauna generally characterized the whole Central Paratethys (Rögl 1998a, b among others). Therefore it is suggested to consider the here described isotope trend as the first step in the evolution of the normal marine enclosed sea Paratethys towards the freshwater Pannonian Lake.

Bicchi et al. (2003) found the signal of the Badenian cooling trend in the Paratethys (Carpathian Foredeep) record stronger than in the Mediterranean. A plausible explanation is to attribute this enhanced cooling in the Paratethys region to the changing circulation. In the Early Badenian heat was transported to the Paratethys region by the warm water current from the lower latitude Mediterranean, while with the reversed circulation in the Late Badenian higher latitude East Paratethys water arrived from the NE. This reversal in circulation changing the heat transport could definitely cause a stronger cooling trend in the Central Paratethys than in the Mediterranean. (Figs. 5, 6).

Late Badenian facies: The increasing stratification indicated by the isotope record is coupled with intensifying accumulation of marine organic matter at the basin floor. The presented data support a model where stratification reaches a certain level by Late Badenian and Sarmatian times at some deeper parts of the Pannonian Basin to enable the burial of enough organic matter to qualify as source rocks of oil or gas. The Zala Basin, a part of the Pannonian Basin in West Hungary, has Badenian sediments with known high total organic content (TOC $\leq$ 0.78) and are considered as a source rock of oil by Clayton and Koncz (1994). Another known occurrence of source rocks and hydrocarbon reservoirs is in the Drava Sava depression (Saftić et al. 2003) in the SW part of the Pannonian Basin.

Reef building organisms, famous for their sensitivity to environmental changes, show decreasing diversity through Badenian times in the Central Paratethys. The final disappearance of corals from the Uppermost Badenian layers (Müller 1984, 1996, personal communication) is suggested to be related to reduced salinity surface water arriving from the East Paratethys in "Konkian" time (Kókay 1985). This level is suspected to correlate to the benthic foraminiferal zones – *"Bolivina-Bulimina"*, "Verarmung Zone" and *"Ammonia beccarii"* zones (Grill 1941; Papp et al. 1978) named after the inbenthic bolivinids and buliminids – and the salinity tolerant *Ammonia* in coastal facies (Fig. 5).

In the Carpathian Foredeep a widespread facies, the so-called " *Limacina*- beds" (old taxonomic name of *Limacina* are "*Spirialis*" and "*Spiratella*"), overlies the evaporitic sediments in NN 6 Badenian (Cicha and Čtyroka 1998; Chira and Dragici 2002 among others). These are calcareous shales with mass occurrence of the planktonic mollusc *Limacina* (Pteropoda) shells at the bedding planes. The preservation of these fragile shells points to oxygen depleted bottom conditions without bioturbation. Similarly *"Limacina"* beds are known from the Oligocene, interbedded in sapropels clearly associated with oxygen depleted environment (Báldi 1986). Poorly oxygenated environments characteristic for the NN 6 Late Badenian could be associated with another characteristic post-evaporitic facies, the radiolarian clays (Barwicz 1999). The formation of siliceous sediments might be the result of carbonate dissolution under such conditions.

Conclusions

The Badenian time span (16.4–13.0 Ma) includes the drastic global cooling following the Mid-Miocene Climatic Optimum. This period of time is the last fully marine interval in the life of the inland sea called Paratethys to become the freshwater Pannonian Lake in few million years. The benthic foraminiferal evidence combined with the stable isotope record provides insight into the paleoceanographic history of this enclosed sea.

1. All benthic foraminiferal proxies indicate increasing organic matter content of sediments and decreasing bottom water oxygen levels by Late Badenian times. Diversity of benthic foraminifera reflects stress, exhibiting a continuous decline from the onset of the NN 6 nannozone to Sarmatian (Fig. 3). The oxygen isotope values show enhancing stratification. The carbon isotope values indicate the accumulation of ^{13}C depleted marine organic matter on the basin floor (Fig. 4). Based upon the observed trends, it is concluded that in the Late Badenian water-mass stratification was strengthened and coupled with the intensified accumulation of marine organic matter at the bottom (Fig. 5).
2. The circulation of an inland sea is strongly linked with climate change. In NN 5 Early Badenian during the Mid-Miocene Climatic Maximum a simple two-layered *antiestuarine* circulation model is suggested based on the presented benthic foraminiferal and stable isotope results. This antiestuarine circulation involved Mediterranean surface water reaching the Central Paratethys Basins, while Central Paratethys deep water flowed back in return. This sort of circulation prevailed during the mid Badenian salinity crisis driven by the positive salt balance necessary also for evaporite formation. In NN 6 Late Badenian, strong *estuarine* circulation is reconstructed based on the isotope values, supporting Kókay's idea (1985). At the end of NN 6 the negative surface water oxygen isotope values are interpreted not just as a result of global cooling, but also as slightly reduced salinities. Such hyposaline surface water arriving from the already brackish East Paratethys clearly indicates an

estuarine sort of connection to any normal marine large water body (Fig. 6).

3. The global cooling following the Mid-Miocene Climatic Optimum (14–13.5 Ma, Böhme 2003) contributed to the change of circulation to the estuarine, besides the effects of tectonic movements changing the connections of the Paratethys basins. Probably the delayed cooling in mid-latitude Europe (Böhme 2003) compared to the deep ocean stable isotope record (14–15 Ma, Zachos et al. 2001) is linked with changes in circulation also. The local Paratethys cooling signal was showed to be stronger than in the Mediterranean (Bicchi et al. 2003), which has been considered in the present work to be the result of the changing heat transport. According to the estuarine circulation model for the Late Badenian (Kókay 1985) the surface water had ceased to flow from the lower latitude Mediterranean with warm water as earlier, but did from the higher latitude East Paratethys (Fig. 6).

Acknowledgements The present study was funded by the postdoctoral grant of the National Science Foundation (OTKA D 042191). I am grateful for the isotope analyses carried out in the laboratory of Utrecht University and for their selfless support over the years. I am especially indebted to Dr. T. Kouwenhoven (Utrecht University) for her altruistic work of commenting and correcting the manuscript, greatly contributing to its present form. I am obliged to express my gratitude to Dr. I. Vetö (Hungarian Geological Institute) for comments concerning the isotope analyses and Dr. P. Müller (Hungarian Geological Institute) for comments on the Badenian stratigraphy and paleogeography. I am grateful to Prof. Dr. G.J. Van der Zwaan, and Dr. J.E. Meulenkamp (Utrecht University) for the fruitful discussions and support. Thanks are due to my close colleague Dr. O. Sztanó (Eötvös University Budapest) for her remarks concerning the present work and my project leader Dr. A. Nagymarosy (Eötvös University Budapest) for sharing his thoughts on stratigraphy. I am grateful for the useful comments and suggestions of Dr. F. Rögl, Dr. E.Turco and an anonymous reviewer.

References

Altenbach AV, Lutze GF, Schiebel R, Schönfeld J (2003) Impact of interrelated and interdependent ecologic controls on benthic foraminifera: an example from the Gulf of Guinea. Palaeogeogr Palaeoclimatol Palaeoecol 197:213–238

Anderson TF, Arthur MA (1983) Stable isotopes of oxygen and carbon and their application to sedimentologic and paleoenvironmental problems. In: Stable isotopes in sedimentary geology. SEPM Short Course N 10, Dallas, pp 1–151

Báldi T (1986) Mid-tertiary stratigraphy and paleogeographic evolution of Hungary. Akadémiai Kiadó Budapest, pp 1–201

Báldi K (1997) Assumed circulation pattern of the Central Paratethys through Badenian (Middle Miocene) times: quantitative paleoeceological analysis of foraminifera from borehole Tengelic-2 (SW Hungary). Acta Geol Hung 40(1):57–71

Báldi K (1999) Taxonomic notes on benthic foraminifera from SW-Hungary Middle Miocene (Badenian) Paratethys. Acta Geol Hung 42(2):193–236

Báldi K, Benkovics L, Sztanó O (2002) Badenian (Middle Miocene) basin development in SW Hungary: geohistory based on quantitative paleobathymetry of foraminifera. Geol Rundsch 91:490–504

Balintoni I, Petrescu I (2002) A hypothesis on the Transylvanian halite genesis. Studia Universitatis Babes-Bolyai Geologia Special issue 1:51–61

Barwicz PW (1999) Badenian Radiolaria from the Krakow area (South Poland). Annales Societatis Geologorum Poloniae 69(3–4):161–172

Berggren WA, Kent DW, Swisher III CC, Aubry M-P (1995) A reviesed Cenozoic geochronology and chronostratigraphy. In: Geochronology time scale and global stratigraphic correlation. SEPM Spec Publication 54:129–212

Bicchi E, Ferrero E, Gonera M (2003) Paleoclimatic interpretation based on Middle Miocene planktonic Foraminifera: the Silesia Basin (Paratethys) and Monteferrato (Tethys) records. Palaeogeogr Palaeoclimatol Palaeoecol 196(3–4):265–303

Böhme M (2003) The Miocene Climatic Optimum: evidence from ectothermic vertebrates of Central Europe. Palaeogeogr Palaeoclimatol Palaeoecol 195(3–4):389–401

Chira C, Draghici D (2002) The calcareous nannoplankton from the Badenian salt and gypsum level in Transylvania. Studia Universitatis Babes-Bolyai Geologia Special issue 1:97–111

Cicha I, Čtyroka J (1998) The Carpathian Foredeep. In: Cicha I, Rögl F, Rupp C, Čtyroka J (eds) Oligocene—Miocene foraminifera of the Central Paratethys. Abh senckenberg naturforsch Ges 649:17

Clayton JL, Koncz I (1994) Petroleum geochemistry of the Zala Basin, Hungary. AAPG Bull 78(1):1–22

Corliss BH (1985) Microhabitats of benthic foraminifera within deep-sea sediments. Nature 314:435–438

Corliss BH, Chen C (1988) Morphotype patterns of Norwegian Sea deep-sea benthic foraminifera and ecological implications. Geology 16:716–719

Daniels Ch von, Ritkowski S (1970) Marines Miozän Orbulina suturalis-Zone in Istrien\Jugoslawien. Göttinger Arbeiten zur Geologie und Palaeontologie 5:31–36

De Stigter HC, Jorissen FJ, Van der Zwaan GJ (1998) Bathymetric distribution and microhabitat partitioning of live (Rose Bengal stained) benthic foraminifera along a shelf to bathyal transect in the southern Adriatic Sea. J Foraminifer Res 28(1):40–65

Den Dulk M, Reichart GJ, Van Heyst S, Zachariasse WJ, Van der Zwaan GJ (2000) Benthic foraminifera as proxies of organic matter flux and bottom water oxygenation? A case history from the northern Arabian Sea. Palaeogeogr Palaeoclimatol Palaeoecol 161(3–4):337–359

Erez J, Luz B (1983) Experimental paleotemperature equation for planktonic foraminifera. Geochim Cosmochim Acta 47:1025–1031

Filipescu S, Girbacea R (1997) Lower Badenian sea-level drop on the western border of the Transylanian Basin: Foraminiferal paleobathymetry and stratigraphy. Geol Carpath 48(5):325–334

Fisher RA, Corbet AS, Williams CB (1943) The relationship between the number of species and the number of individuals in a random sample of an animal population. J Anim Ecol 12:42–58

Flower BP, Kennett JP (1994) Middle Miocene ocean-climate transition: high-resolution oxygen and carbon isotopic records from the Deep Sea Drilling Project Site 588A, Southwest Pacific. Paleoceanography 8(6):811–843

Fontanier C, Jorissen FJ, Licari L, Alexandre A, Anschutz P, Carbonel P (2002) Live benthic foraminiferal faunas from the Bay of Biscay: faunal density, composition and microhabitats. Deep Sea Res I 49:751–785

Geary DH, Rich J, Valley JW, Baker K (1989) Stable isotope evidence of salinity change: Influence on the evolution of melanopsid gastropods in the late Miocene Pannonian Basin. Geology 17:981–985

Gebhardt H (1999) Middle to Upper Miocene benthinic foraminiferal paleoecology of the Tap Marls (Alicante Province, SE Spain) and its paleoceanographic implications. Palaeogeogr Palaeoclimatol Palaeoecol 145:141–156

Gonera M, Peryt TM, Durakiewicz T (2000) Biostratigraphical and paleoenvironmental implications of isotopic studies (^{18}O, ^{13}C) of Middle Miocene (Badenian) foraminifers in the Central Paratethys. Terra Nova 12:231–238

Gontsharova IA (2001) Tarkhanian and Chokrakian of the Eastern Paratethys, state of knowledge and correlation. Ber Inst Geol Paläont K-F Univ Graz 4:14–22
Grill R (1941) Stratigraphische Untersuchugen mit Hilfe von Microfaunen im Wiener Becken und den benachbarten Molasse-Anteilen. Oel und Kohle 31(15):595–603
Halmai J, Jámbor Á, Ravasz-Baranyai L, Vetõ I (1982) Geological results of the borehole Tengelic-2. (in Hungarian also). Ann Inst Geol Publ Hung LXV:93–138
Hámor G (1970) A Kelet-Mecsek-i miocén (The Miocene of the E Mecsek Mts., SW Hungary). Ann Geol Inst Hungary 53:1–484
Harzhauser M, Piller WE, Steininger FF (2002) Circum-Mediterranean Oligo-Miocene biogeographic evolution—the gastropods' point of view. Palaeogeogr Palaeoclimatol Palaeoecol 183:103–133
Holcová K (1999) Postmortem transport and resedimentaion of foraminiferal tests: relations to cyclical changes of foraminiferal assemblages. Palaeogeogr Palaeoclimatol Palaeoecol 145:157–182
Ivanov D, Ashraf AR, Mosbrugger V, Palamarev E (2002) Palynological evidence for Miocene climate change in the Forecarpathian Basin (Central Paratethys, NW Bulgaria). Palaeogeogr Palaeoclimatol Palaeoecol 178:19–37
Jannink NT, Van der Zwaan GJ, Zachariasse WJ (1998) Living (Rose Bengal stained) foraminifera from an upwelling environment: the continental margin south of Karachi, Arabian Sea. Deep Sea Res I 45:1483–1513
John AWG (1987) The regular occurrence of Reophax scottii Chaster, a benthic foraminiferan, in plankton samples from the North Sea. J Micropaleontol 6(2):61–63
Jorissen FJ (1987) The distribution of benthic foraminifera in the Adriatic Sea. Marine Micropaleontol 12:21–48
Jorissen FJ, De Stigter HC, Widmark JGV (1995) A conceptual model explaining benthic foraminifera microhabitat. Marine Micropaleontol 26:3–15
Kaiho K (1994) Benthic foraminiferal dissolved-oxygen index and dissolved oxygen levels in the modern ocean. Geology 22:719–722
Kaiho K (1999) Effect of organic carbon flux and dissolved oxygen on the benthic foraminiferal oxygen index (BFOI). Marine Micropaleontol 37:67–76
Kennett JP (1985) Miocene to Early Pliocene oxygen and carbon isotope stratigraphy in the Southwest Pacific, Deep Sea Drilling Project Leg 90. In: Kennett JP, von der Borch CC et al (eds) Initial reports of the deep sea drilling project 90:1383–1411
Kókay J (1985) Central and Eastern Paratethys interrelations in the light of late Badenian salinity conditions. Geol Hung Ser Paleontol 48:7–97
Kouwenhoven TJ, Van der Zwaan GJ (2004) A reconstruction of late Miocene Mediterranean circulation patterns using benthic foraminifera. Palaeogeogr Palaeoclimatol Palaeoecol (in press)
Krzywiec P (2001) Contrasting tectonic and sedimentary history of the central and eastern parts of the Polish Carpathian foredeep basin—results of seismic data interpretation. Marine Petrol Geol 18:13–38
Luczkowska E (1979) Biostratigraphic correlation of the Wieliczien substage (Middle Badenian) in Poland and in the Vienna Basin. Ann Geol Pays Hellen 1979 (II): 717–726 VII International Congress on the Mediterranean Neogene Athens 1979
Marinescu F, Marunteanu M (1990) La paléogéographie au niveau du sel Badénien en Roumanie. (The paleogeography of the Badenian evaporite level in Romania. In French). Geol Zborník - Geol Carpathica Bratislava 41(1):49–58
Martini E (1971) Standard Tertiary and Quaternary calcareous nannoplankton zonation. Proc of the II Planktonic Conf Roma 1970, pp 739–785
Martini E (1990) The rhinegraben system, a connection between northern and southern seas in the European Tertiary. Veröff Übersee-Mus A10 Bremen pp 83–98
Mátyás J, Burns SJ, Müller P, Magyar I (1996) What isotopes can say about salinity? an example from the Late Miocene Pannonian Lake. Palaios V:31–39
Mészáros N, Nicorici E, Filipescu S (1989) Le nannoplancton des dépôts Néogénes saliferes traversés par les forages executés aux environs de la ville Turda. Studia Univ Babes - Bólyai Geologia - Geographia XXXIV:2
Meulenkamp JE, Sissingh W (2003) Tertiary palaeogeography and tectonostratigraphic evolution of the Northern and Southern Peri-Tethys platforms and the intermediate domains of the African-Eurasian convergent plate boundary zone. Palaeogeogr Palaeoclimatol Palaeoecol 196:209–228
Miller AR (1983) The Mediterranean Sea A Physical Aspects. In: Ketchum BE (ed) Estuaries and enclosed Seas, Ecosystems of the world 26. Elsevier, Amsterdam, pp 219–239
Miller KG, Feigenson MD, Wright JD, Clement BM, (1991) Miocene isotope reference section, DSDP Site 608: An evaluation of isotope and biostratigraphic resolution. Paleoceanography 6:33–52
Moore TC, Pisias NG, Keigwin ID (1981) Ocean basin and depth variability of oxygen isotopes in Cenozoic benthic foraminifera. Marine Micropaleontol 6:465–481
Müller P (1984) Decapod Crustacea of the Badenian. Geol Hung Ser Pal 42:1–317
Müller P (1996) Middle Miocene decapod Crustacea from southern Poland. Prace Muzeum Ziemi (Prace paleozoologiczne) 43:3–16
Murray JW (2001) The niche of benthic foraminifera, critical thresholds and proxies. Marine Micropaleontology 41:1–7
Nagymarosy A (1980) A magyarországi bádenien korrelációja nannoplankton alapján. (Correlation of the Hungarian Badenian based on Nannoplankton. In Hungarian). Földtani Közlöny 110: 206–245
Nagymarosy A (1982) Badenian-Sarmatian nannoflora from the borehole Tengelic-2. In: Halmai J, Jámbor Á, Ravasz-Baranyai L, Vetö I (eds): Geological results of the borehole Tengelic-2. (in Hungarian and English). Ann Inst Geol Publ Hung LXV:145–186
Nagymarosy A (1985) The correlation of the Badenian in Hungary based on Nannoflora. Annales of the Eötvös University Budapest Sect Geol XXV 1983:33–86
Papp A, Cicha I (1978) Definition der Zeitenheit Miozän. (Definition of the Miocene - Badenian.) In: Papp A et al (eds) Chronostratigraphie und Neostratotypen. Miocene of the Central Paratethys (in German) 6 M_4, Badenien pp 47–49
Papp A, Cicha I, Seneš J, Steininger F (1978) Chronostratigraphie und Neostratotypen. Miozän der Zentralen Paratethys (in German). 6: M_4, Badenien (Moravien, Wielicien, Kosovien) Bratislava, pp 1–594
Peryt D (1997) Calcareous Nannoplankton Stratigraphy of the Middle Miocene in the Gliwice Area (Upper Silesia, Poland). Bull Polish Acad Sci Earth Sci 45(2–4):119–131
Por FD, Dimentman C (1985) Continuity of the Messinean Biota in the Mediterranean Basin. In: Stanley DJ, Wezel FC (eds) The geological evolution of the Mediterranean. Springer, Berlin Heidelberg New York, pp 545–557
Rathburn AE, Corliss BH, Tappa KD, Lohmann KC (1996) Comparison of the ecology and stable isotopic compositions of living (stained) benthic foraminifera from the Sulu and South China Seas. Deep-Sea Res I 43(10):1617–1646
Rögl F (1996) Stratigraphic correlation of the Paratethys Oligocene and Miocene. Mitt Ges Geol Bergbaustud Österr Wien 41:65–73
Rögl F (1998a) Paratethys Oligocene-Miocene Stratigraphic Correlation. In: Cicha I, Rögl F, Rupp C, Ctyroka J (eds) Oligocene – Miocene foraminifera of the Central Paratethys. Abh senckenberg naturforsch Ges 649:3–7
Rögl F (1998b) Palaeogeographic considerations for Mediterranean and Paratethys Seaways (Oligocene to Miocene). Ann Naturhist Mus Wien 99(A):279–310
Rögl F, Müller C (1976) Das Mittelmiozän und die Baden-Sarmat Grenze in Walbersdorf (Burgenland). Ann Naturhist Mus Wien 80:221–232

Rögl F, Steininger FF (1983) Vom Zerfall der Tethys zu Mediterran und Paratethys. Die neogene Palaeogeographie und Palinspastik der zirkum-mediterranen Raumes. Ann Naturhist Mus Wien 85(A):135–163

Rögl F, Steininger F, Müller C (1978) Middle Miocene salinity crisis and paleogeography of the Paratethys (Middle and Eastern Europe). Initial reports of the Deep Sea Drilling Project Washington XLII(1):985–990

Rögl F, Spezzaferri S, Ćorić S (2002) Micropaleontology and biostratigraphy of Karpatian-Badenian transition (Early-Middle Miocene boundary) in Austria (Central Paratethys). Courier Forsch. Inst. Senckenberg, Frankfurt am Main 236:47–67

Rosoff DB, Corliss BH (1992) An analysis of Recent deep-sea benthic foraminiferal morphotypes from the Norwegian and Greenland seas. Palaeogeogr Palaeoclimatol Palaeoecol 91:13–20

Ross DA (1983) The Red Sea. In: Ketchum BE (ed) Estuaries and Enclosed Seas. Ecosystems of the world 26. Elsevier, Amsterdam, pp 293–306

Saftić B, Velić J, Sztanó O, Juhász Gy, Ivković Ž (2003) Tertiary Facies, Source Rocks and Hydrocarbon Reservoirs in the SW Part of the Pannonian Basin (Northern Croatia and South-Western Hungary). Geol Croatica 56(1):101–122

Schwarz T (1997) Lateritic bauxite in central Germany and implications for Miocene paleoclimate. Palaeogeogr Palaeoclimatol Palaeoecol 129:37–50

Seidenkrantz MS, Kouwenhoven TJ, Jorissen FJ, Shackleton NJ, Van der Zwaan GJ (2000) Benthic foraminifera as indicators of changing Mediterranean-Atlantic water exchange in the late Miocene. Marine Geol 163(1–4):387–407

Sprovieri M, Bellanca A, Bonanno A, Mazzola S, Neri R, Patti B, Manta DM, Pueyo JJ, Pujol CT (1999) Paleogeographic changes in the Neogene Mediterranean: Geochemical and Micropaleontological evidence. In: Europian Union of Geosciences conference abstracts, EUG 10, Journal of conference abstracts. 4, p. 209. Cambridge Publications.

Steininger FF, Rögl F (1984) Paleogeography and palinspastic reconstruction of the Neogene of the Mediterranean and the Paratethys. In: Dixon JE, Robertson AHF (eds) The geologic evolution of the Eastern Mediterranean. The Geological Society Blackwell Scientific Publications, pp 659–668

Steininger FF, Bernor RL, Fahlbusch V (1990) European neogene marine\continental chronologic correlations. In: Lindsay EH, Fahlbusch V, Mein P (eds) European neogene mammal chronology. Plenum, New York, pp 15–46

Studencka B, Gontsharova IA, Popov SV (1998) The bivalve faunas as a basis for reconstruction of the Middle Miocene history of the Paratethys. Acta Geol Polonica 48(3):285–342

Swart PK, Price RM, Greer L (2001) The relationship between stable isotopic variation (O, H and C) and salinity in waters and corals from environments in South Florida: implications for reading the paleoenvironmental record. Bull Am Paleontol 361:17–29

Szczechura J (1982) Middle Miocene foraminiferal biochronology and ecology of SE Poland. Acta Palaeontol Polonica 27(1–4):3–44

Szczechura J (1996) Indo-pacific affinities of the Paratethys contested. Acta Palaeontol Polonica 41(2):146–148

Švabenická L (2002) Calcareaous nannofossils of the Upper Karpatian and Lower Badenian Deposits in the Carpathian Foredeep, Moravia (Czech Republic). Geologica Carpathica 53(3):197–210

Van der Zwaan GJ, Jorissen FJ (1991) Biofacial patterns in river induced shelf anoxia. In: Tyson RV, Pearson TH (eds) Modern and Ancient Continental Shelf Anoxia. Geol Soc London Spec Publ 58:65–82

Van der Zwaan GJ, Jorissen FJ, Verhallen PJJM, Daniels Ch. von (1986) Atlantic-European Oligocene to recent Uvigerina. Utrecht Micropal Bull 35:1–237

Van der Zwaan GJ, Jorissen FJ, De Stigter HC (1990) The depth dependency of planktonic\benthic foraminiferal ratios: constraints and applications. Marine Geol 95:1–16

Vennemann TW, Hegner E (1998) Oxygen, strontium, and neodynium isotope composition of fossil shark teeth as a proxy for the paleoceanography and paleoclimatology of the Miocene northern Alpine Paratethys. Palaeogeogr Palaeoclimatol Palaeoecol 142:107–121

Vergnaud-Grazzini C (1985) Mediterranean Late Cenozoic stable isotope record: stratigraphic and paleoclimatic implications. In: Stanley DJ, Wezel FC (eds) The geological evolution of the Mediterranean. Springer, Berlin Heidelberg New York, pp 413–451

Williams CB (1964) Patterns in the balance of nature. Academic, London, pp 1–324

Zachos J, Pagani M, Sloan L, Thomas E, Billups K (2001) Trends, rythms and aberrations in the global climate 65 Ma to present. Science 292:686–693

View publication stats